

# Opportunity for Regulating the Collective Effect of Random Expansion with Manifestations of Finite Size Effects in a Moderate Number of Finite Systems

Włodzimierz Kozłowski\*

*Institute of Biocybernetics & Biomedical Engineering  
of The Polish Academy of Sciences, Trojdena 4, 02-109 Warsaw, Poland  
(Dated: March 22, 2022)*

One reports computational study revealing a set of general requirements, fulfilling of which would allow employing changes in ambient conditions to regulate accomplishing the collective outcome of emerging active network patterns in an ensemble of a moderate number of finite discrete systems. The patterns within all these component systems emerge out of random expansion process governed by certain local rule. The systems modeled are of the same type but different in details, finite discrete spatial domains of the expansion within the systems are equivalent regular hexagonal arrays. The way in which elements of a component system function in the local information transmission allows dividing them into two classes. One class is represented by zero-dimensional entities coupled into pairs identified at the array sites being nearest neighbors. The pairs preserve their orientation in the space while experiencing conditional hopping to positions close by and transferring certain information portions. Messenger particles hopping to signal the pairs for the conditional jumping constitute the other class. Contribution from the hopping pairs results in finite size effects being specific feature of accomplishing the mean expected network pattern representing the collective outcome. It is shown how manifestations of the finite size effects allow using changes in parameters of the model ambient conditions of the ensemble evolution to regulate accomplishing the collective outcome representation.

PACS numbers: 05.10.-a, 05.60.-k, 89.75.Fb, 45.70.Qj

Keywords: collective effects, regulation, discrete systems, finite size effects

## I. INTRODUCTION

This study contributes to a search for methods of *regulating* the collective outcome of assembly processes taking place in an ensemble of a moderate number  $M$  of finite complex systems, of the same type but different in details, evolving simultaneously and independently, under influence of stochastic factors within equivalent finite spatial domains and in the same ambient conditions. The finite discrete spatial domains are equivalent regular arrays in all the component systems. Information transmission processes within these domains result in manifestations represented by various patterns of expanding spatial regions specified with the same feature in all the systems at each stage of the process. One assumes that these regions specified within all the component systems affect simultaneously certain receiver system. Moreover, differences between contributions, which distinct component systems have to the effect of their influence on the receiver system, are attributed only to differences between spatial arrangements of the regions specified within these component systems. Accordingly, spatial arrangements of these regions within all the systems correspond to the receiver system transformation that manifests itself as a *collective effect* (CE) at each stage of the process. Thus the receiver system recognizes collective outcome of evolution processes within all the component systems. One also assumes that all the component systems contribute

to the collective effect in the equivalent conditions. For the reasons just noted, the CE can be represented by certain pattern of distinguished regions within a spatial domain being equivalent to the domain of a component system. Changing certain values parameterizing the ambient conditions of evolution of all the component systems is the way in which regulation of the collective effect is under consideration here.

In course of this study we have found that a prerequisite for following this way is presence of *finite-size effects* (we use abbreviation, F-SE) i.e. specific features of the CE accomplishment which result from realizing the local information transfer in the component systems of the evolving ensemble by one dimensional, finite-size elements able to change their positions in finite discrete space while transmitting certain signals between their ends and preserving their orientation in the space. The signal is considered as finite portion of information transmitted discretely between an element ends. Accordingly, each such element is represented by the pair of its ends only, one end that only sends a signal and the other receiving it. These ends coincide with sites of the regular array which are nearest neighbors. Hopping of the pair to a separate position close by requires obeying certain stochastic condition. Whole the pattern within each component system is being accomplished at each step of the evolution and can be composed only of sites being destinations for the receiving ends of the pairs that have experienced hopping at this step. This results in high diversity of the patterns which manifests itself in appearance of rugged islands in course of a component system evolution initiated from a single cluster; this specific diver-

---

\*Electronic address: wlodekak@ibb.waw.pl

sification is a prerequisite for appearance of the F-SE. It has been also found that manifestations of the F-SE allow regulating the CE accomplishment effectively, in the way just mentioned, if elements constituting other class signal the pairs to perform the conditional hopping. This class encompasses elements represented by zero-dimensional entities transferring the information portions by hopping between closest neighbor sites. The way of modeling the local information transfer just mentioned is explained in Section II and algorithms of modeling the conditional information transfer are presented in Section III. This has been assumed as simplest model allowing the manifestations of effects being the subject investigated in course of this research (this is elucidated in Sections IV and VI).

Remarkable manifestations of the *finite-size effects*, *finiteness and discreteness* have appeared indispensable to allow regulating the CE accomplishment. The number,  $M$  of the component systems affects usefulness of these manifestations for the regulation. The term *moderate*  $M$  used hereafter means:  $M$  is so large that the collective effect is accomplished reliably with certain specific features and  $M$  is so small that all diverse specific manifestations attributed to the discreteness, finiteness and transfers resulting in the finite-size effects are remarkable and can be easily identified in the CE. The way of estimating the lower bound  $M_0$  of the  $M$  being moderate and role of other values parameterizing the model ambient conditions are presented in Section IV. Criterion of detecting the upper bound,  $M_1$  to the value  $M$  considered as being moderate and its role are explained in Sections VIB3, VIC).

One of the motives for doing this research is the necessity in predicting the opportunity for regulating the collective effect emerging out of evolution of an ensemble of systems of nanoelements that are assembling quasi two-dimensional functional networks over prepatterned surfaces (for the purpose of modeling this process, the nanoelements can be represented by pairs of their ends only in the way alluded to previously). This task may be considered as being relevant to low cost process of self-assembling nanostructured functional materials (this is the so called *bottom-up method*) that are expected to be applied as sensors, electric field emitters stimulating living tissues and as other active covers. Then, an electron would be usually the signal transmitted by the nanoelements and this explains the convention of identifying them as nanowires. The short mobile nanowires would differ from one another in length and conductivity, and the conduction would influence binding other elements at their ends. A number of them would be tethered, either temporarily or permanently, by elements of the surface texture that would constrain freedom of their displacements and the differences between the nano-wires would contribute to the system randomness. One may suggest a number of candidates for the material components of such systems. For example, properties of single-walled carbon nanotube conductors [1] (see also <http://cnanotech.com>) allow considering their short

intervals as candidates for the short nanowires. The short nanotube intervals can emit electric field from their ends, form stable colloidal suspension in water [2] and can be adsorbed spontaneously to a gold surface [3]. Possibility of fabricating multivalent receptors on the gold nanoparticle scaffolds [4] seems to open the opportunity for employing them to recognize elements self-assembling into the network. Moreover, gold nanocrystals can self-assemble into ordered hexagonal texture of the surface [5] and electron transfer appears to be engaged into their interactions with fullerene particles [6]. This reveals feasibility of a material system evolution being relevant to the model process reported here. Let us note, however, that general character of the model assumptions made in this research may make the presented approach useful for studying other physical processes also.

A computational study of the opportunity for regulating the collective effect emerging out of the ensemble of evolving complex systems can be carried on by simulating the model process proposed here. We employ the known idea [7, 8, 9, 10] of considering signals being finite portions of information about certain generalized model feature transported in discrete way between sites of a finite discrete space (the space is represented here by finite regular hexagonal lattice). Appearance of that model feature at a site is indicated by covering this site. Thus a pattern of covered sites within spatial domain of a system represents effect of the system evolution.

It is specific to this model that the scheme of covering the sites is assumed so as to represent effectively the underlying transport mechanisms resulting, eventually, in the finite-size effects. For this purpose we adapt our method of discrete displacements, within frame of which hopping pairs of zero-dimensional entities have been employed to simulate effects of information transmission relevant to turbulent transport and, then, agreement with available experimental results has been demonstrated [9]. Here, the collective effect is represented by the pattern being mean expected form of the patterns emerging under equivalent conditions, simultaneously and independently (in parallel) in all systems constituting the ensemble.

In this work, one investigates random expansion process (REP) as Markov process of covering sites of finite regular hexagonal array. States of the REP at stages  $T$  are finite random sets (FRS),  $F(T) = \{A_i(T), i = 1, 2, \dots, M\}$ . The realizations  $A_i(T)$  develop simultaneously and independently in the same model ambient conditions. Accomplishing of the model collective effect is represented by sequence of patterns  $\int F(T)$ , each of which is mean expected form of all the  $A_i(T)$  and computed as mean measure set (MMS) after known algorithm [11] briefly reported in the Appendix.

Characteristics of the MMS evolution pattern are presented in Section V. Specific, predictable changes in the MMS evolution patterns, which result from varying certain parameters of the model ambient conditions, have been recognized as features attributed to the finite-size

effects modeling. They reveal a possible way of searching for a method of regulating the collective effect emerging out of a material system ensemble for which the process underlying evolution of the ensemble may be adequately represented by the REP. These results are presented and discussed in Section VI.

## II. METHOD OF MODELING THE LOCAL INFORMATION TRANSFER

The way of modeling the mechanism of information transfer in each realization  $A_i$  evolving from a stage  $T$  to  $T + 1$  can be elucidated by considering certain idealized physical system. Let us assume that the system consists of short nanowires, transferring signals while hopping to positions close by, and of certain complex molecules occupying all sites of the finite hexagonal array representing texture of a prepatterned surface. Moreover, transmission of the signal changes binding properties at the nanowire ends and this can affect behavior of the complex molecules occupying sites coinciding with these ends. With the purpose to model effects produced by the nanowires, we generalize our approach [9] used previously for modeling the contribution which certain finite-size elements representing organized fluid streams and structures have to the collective effect of transport processes in the turbulent shear flow. In accordance with this approach, employed to situation being considered here, the finite-size elements transferring the signals are modeled as pairs of neighbor sites  $(x, y)$  that transmit a signal from  $x$  to  $y$  while hopping effectively to a position  $(x', y')$  close by. This effective hoppings are realized so that information portion about orientation of two neighbor sites coupled into a pair is transferred from the position  $(x, y)$  to  $(x', y')$  (see the triplet of patterns in the bottom of Fig. 1a). Generally, each pair of neighbor sites can be considered coinciding with both ends of a model nanowire. Let us explain in this connection that the model being presented should not be considered literally: The model is effective in character, i.e. local model processes can represent cumulative outcome of all possible local actual realizations allowed in certain ambient conditions by the space configuration (here, hexagonal array) and related to one step of the model evolution. Further we explain spatiotemporal aspect of the effective modeling and thus reveal way of representing diversity of possible events which results from participation of the hopping pairs in the information transmission.

The pattern identifying the realization  $A_i(T)$  is composed of sites covered at the stage  $T$  only. The covering of a site represents activation of a complex molecule at the site in the idealized physical system considered. In this system, each molecule activated sends identical messenger particles to all its nearest neighbors. In the computational model, each messenger particle is represented by a signal  $C$  being the same for each site covered from which the  $C$  is sent. Accordingly, each site occupied by

such activated molecule is identified as a site with distributable feature  $C$ . One assumes that each molecule being active at a stage  $T$  sends unconditionally the messenger particles  $C$  to all its nearest neighbors at the step of evolution, from  $T$  to  $T + 1$ , and thus loses its activity. A molecule can become active at the stage  $T + 1$  only in result of a process identified hereafter as *transferring the molecule activity* by a nanowire at the step of evolution from  $T$  to  $T + 1$ ; this process is elucidated below. For first, we explain spatial aspect of the effective modeling of the local information transfer and this will help us to explain subsequently its temporal aspect.

One assumes that the messenger particle  $C$  coming to a molecule (either activated or not) from a nearest neighbor one can be effectively redirected to any molecule being the nearest neighbor of this intermediate one (see Fig. 1a). In virtue of the effective modeling alluded to previously, we represent contribution that these local redirection events have to effects of the transport process diversity as local cumulative result of the all possible model events of the redirection. Note that differences between the model events contributing to the local cumulative result concern only ways of the component redirections and are attributed to the space topology identified as regular hexagonal tiling. As no direction in this regular array is distinguished, the local cumulative result can be assigned to a virtual situation in which an active molecule would send for six messenger particles to each its nearest neighbor molecule that would redirect them, for one, to each of its six nearest neighbor molecules. The redirection does not cause any changes of the molecule redirecting the particles but the messenger particles redirected acquire new feature allowing them activating each nanowire whose sending end coincides with a site occupied by a molecule being nearest neighbor of the one that has redirected the particle. This new feature is considered as enhancement of the signal  $C$  due to the redirection and we denote the signal enhanced as  $C_r$ . Note that arrangement of sites into the hexagonal array allows activating nanowires at the six initial positions by one messenger particle  $C_r$  achieving the site coinciding with their overlapping sending ends. Here, for clarity, we continue the explanation for example of possible behavior of a nanowire at one initial position (sufficient conditions to be obeyed for activating those nanowires as well as nature of the effective modeling the transport process that engages them are revealed hereafter). A nanowire activated by the signal  $C_r$  delivered to its sending end can act as a carrier hopping to a position close by while transmitting certain signal  $Q$  emitted from its sending end toward the receiving one (see Fig. 1a). The  $C_r$  does not affect the complex molecule at the site coinciding with the sending end of the nanowire. Moreover, state of this molecule, which can be intact or activated, has no effect on activating the nanowire by the  $C_r$ . The  $Q$  itself is *not* a molecule activation signal, transmission of the  $Q$  by the nanowire is required to change binding properties at the nanowire ends: then the sending end can recognize

a molecule that was active at a stage  $T$  and this allows reception of the nanowire at its receiving end by the intact molecule occupying the same site as this end at the stage  $T + 1$ . This reception makes this molecule active at the stage  $T + 1$ . The reception of a single active nanowire is sufficient to activate the molecule. The molecule that can be activated in the way just presented will be identified hereafter as *target molecule* occupying the *target site*. In accordance with assumptions alluded to previously, an active nanowire can experience hopping only to a position identified by a pair of neighbor sites so orientated in space as the pair of neighbor sites representing the nanowire at its initial position. Moreover, one assumes that directions of the nanowire displacements agree with direction of transmitting the  $Q$ , from the nanowire sending end to the receiving one. Accordingly, there are five such positions close by which are identified by pairs of neighbor sites that do not coincide with any of the two sites identifying the initial position (see Fig. 1a). Let us recall that, within frame of the information transfer representation being considered, the state of transmitting the signal  $Q$  and hopping of the active nanowire take place at one step of evolution which is elementary unit of time here. Therefore, change of binding properties at the active nanowire ends due to appearance of the nanowire in the state of transmitting the signal  $Q$  concerns also the nanowire at its initial position. The nanowire action following the change in binding properties of its ends can be considered as direct transfer of the molecule activity. Eventually, we consider an active nanowire that can transfer directly the molecule activity at any of the six positions identified as *destination positions*. Thus it can contribute to the information transmission stream that is initiated by emitting the messenger particles,  $C$  and occurs at each step of the evolution.

Let us explain in this connection the nature of the effective modeling of the local transfer realized by the nanowires. Our approach is like the one used in the case of the messenger particle redistribution elucidated here previously. Contribution that the local hoppings of the active nanowires have to effects of spatial diversity in the transfer processes for one step of the evolution, from the  $T$  to  $T + 1$ , is modeled as result of a virtual event in course of which six nanowires are activated at one initial position, experience hopping and are able to transfer directly the molecule activity at the six destination positions respectively (see Fig. 1a). Let us note that the pattern just sketched for example of a nanowire activated at one initial position remains the same for each of six possible initial positions at which nanowires with coinciding sending ends are activated by the  $C_r$  (one messenger particle  $C_r$  is sufficient to activate nanowires at all the six initial positions). Certain ambient gradient can constrain number of the initial positions at which activation of the nanowire is allowed (we elucidate that opportunity hereafter).

Temporal aspect of the effective modeling may be explained by using a notion of virtual multistate of a com-

plex molecule that has been activated at a stage  $T$ . At a step of the effective model process, it is thought as appearing in virtual three-state: the state of becoming intact by emitting the messenger particle  $C$ , the state of being probed by sending end of a nanowire at its destination position (then, available information about molecule activity refers to the stage  $T$  only), the state of remaining intact or becoming active for the future by accepting receiving end of the nanowire. Eventually, the molecule appears in the single state of being intact or activated at the stage  $T + 1$ . Accordingly, participation of the messenger particles and the model nanowire in the local information transfer is related only to the virtual three-state of the complex molecule as alluded to previously (this refers also to virtual bi-state of the complex molecule being intact at the  $T$  and thus unable to emit the particle  $C$ ).

The *effective* model pattern of the local information transfer realized by the nanowires can be alternatively represented by a formal scheme in which information about nanowire orientation,  $(x, y)$  in the discrete space and the signal  $Q$  are coupled into one transferable information portion denoted as  $Q_{(x,y)}$  (see Fig. 1b). Within frame of this formal scheme, activation of a nanowire by the  $C_r$  results in appearance of the information portions,  $Q_{(x,y)}$  and their distribution to the six target sites being the nearest neighbor sites of the  $x'$  identified as a site nearest the pair  $(x, y)$  in the direction from  $x$  to  $y$ . Thus, this  $x'$  may be imagined as a node redirecting the hopping information portions,  $Q_{(x,y)}$  toward all its closest neighbors. This imaginary event will be identified hereafter as act of *hopping-distribution*. In accordance with role of the signal  $Q$ , which has been explained here previously, delivering the  $Q_{(x,y)}$  in the way of the hopping-distribution to each respective target site allows covering it at a stage  $T + 1$  if its nearest neighbor site, so oriented in respect to it as  $x$  is oriented in respect to  $y$ , has been covered at the stage  $T$  of the evolution. The  $Q_{(x,y)}$  will be identified hereafter as information portion about covering such target site at  $T + 1$  (we will also use the phrase a *signal about covering a target site* to identify the  $Q_{(x,y)}$ ). The scheme of the hopping-distribution is used, as more convenient, for presenting algorithms of the conditional information transfer.

Let us recall that we model evolution that is random process and the scenario presented is to be supplemented by introducing certain stochastic condition. Note, in this connection, that one of the outcomes of redirecting the messenger particle  $C$  is reflecting this particle acquiring the property  $C_r$  back to the molecule sending it. One may consider a process allowing only this way of redirection. Then, only the nanowires whose sending ends coincide with the site occupied by the molecule sending the  $C$  can be activated by the messenger particle reflected as the  $C_r$ . This scenario corresponds to the process that can be considered as particular case of the process presented here previously. In this reduced scenario, the hopping-distribution would be the only model mechanism of the

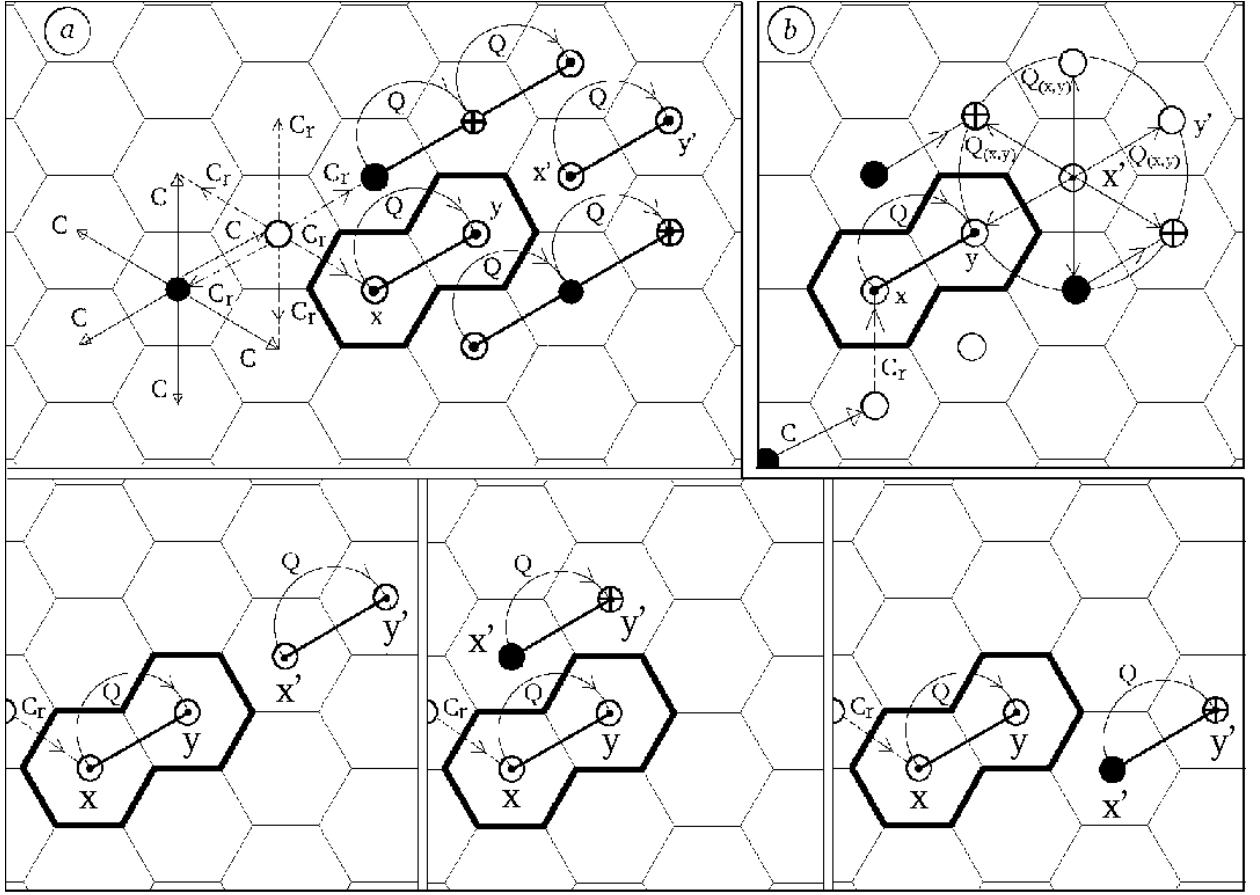


FIG. 1: Effective modeling a path of the local information transfer in a component system  $A_i$  for one step of the evolution, from  $T$  to  $T+1$ . (a) The nanowires represented by pairs of neighbor sites are activated by the messenger particle  $C_r$  and experience hopping while being in state of transmitting a signal  $Q$  (for the picture clarity, hopping from only one initial position of the nanowire is depicted). Three patterns at the bottom illustrate examples of the information transfer model events contributing to the virtual effective model event depicted above. (b) Alternative representation of the local information transfer example: the  $Q$  and the information about nanowire orientation,  $(x, y)$  are considered as coupled into one transferable information portion,  $Q_{(x,y)}$ ; note that activation of the nanowire does not depend on direction, from which the  $C_r$  has come (see Section II). In all the patterns: Black circles identify sites covered at stage  $T$ ; the symbol,  $\oplus$  detects sites that can be covered for the  $T+1$  in result of the example event depicted; other sites which are indicated by the circles,  $\circ$  are not covered at the stage  $T$  and will not be covered for the  $T+1$  in result of the example event depicted (those uncovered sites, which coincide with ends of the nanowires shown, are indicated by  $\odot$ ).

information transfer (we call it, direct transfer process (DTP) whereas the process encompassing the complete distribution of the  $C_r$  is identified as indirect transfer process (ITP)). Note, however, that transfer of the information portion about orientation of a pair of neighbor sites in the discrete space is specific feature of the model process in both the scenarios, ITP and DTP. For that reason, one assumes a stochastic condition of occurrence of the information transfer realized by the active nanowires: in terminology used in the formal model, this is condition of occurrence of the hopping-distribution. Moreover, assuming the agreement between directions of an active nanowire displacements and direction of transmitting the  $Q$ , from the nanowire sending end toward the receiving one, suggests expressing this condition as relationship between a value characterizing local, time independent ef-

fect of stochastic factors and certain ambient gradient of a determined forcing factor. Accordingly, we assume a constant value parameterizing one determined ambient gradient of a forcing factor imposed onto all the ensemble systems in course of the evolution. Note that using a gradient of the forcing factor to express the stochastic condition will result in constraining a number of the initial positions at which activation of a nanowire is allowed. Value of the gradient pertaining to expression of this condition can be assumed so that evolution results in stable state without further growth of the lattice area covered (see Section IV A, V).

### III. ALGORITHMS OF CONDITIONAL LOCAL TRANSFER

#### A. Spatial domain

All the independent realizations,  $A_i(T)$  evolve in the same spatial domain under influence of stochastic factors and with the same process parameters characterizing the model ambient conditions. The spatial domain is a finite discrete space  $\chi = \{x_k, k = 1, 2, \dots, N\}$  constituted by  $N < \infty$  nodes of a regular triangular grid embedded into a plane so as to fill in a square with the sides of  $1 \times 1$ . This grid has largest density of nodes among all possible grids with the same value of the smallest distance between the nodes [12]. Each of the embedded nodes is situated at center of a regular hexagon of the honeycomb array covering the square. A node as well as the hexagon assigned to it are identified also with the term "site" (the terms "node" and "site" are used interchangeably here). A node  $x$  and its vicinity  $V_x$  composed of its nearest neighbors  $y_1, y_2, \dots, y_6$  are shown in Fig. 2a (the  $V_x = \{y_j, j = 1 \div 6\}$  together with the  $x$  are denoted as neighborhood  $S_x$ ). The  $A_i(T)$  are represented by patterns composed only of sites covered at stage  $T$  of the evolution.

#### B. Direct transfer process REP-DTP

We employ the scheme of the hopping-distribution (see Section II) to present algorithm of *conditional* covering the sites. Let a node  $x$  shown in Fig. 2b be covered in the realization  $A_i$  at a stage  $T$ ,  $x \in A_i(T)$  (symbol  $\in$  is read "is an element of"). This site is considered active and sends signals  $C$  that can be reflected only by the neighbor sites, as signals  $C_r$ , back to the  $x$ . Accordingly to the assumption put forward in Section II, a model nanowire represented by the pair of neighbor sites at its initial position,  $(x, y_j)$  with  $y_j \in V_x$ , can be activated by the signal  $C_r$ . Index,  $j$  identifies here orientation of the pair within the  $S_x$  and pair of indices,  $jl$ , with  $l = 1, 2, \dots, 6$ , is used to indicate all target sites, to which the information portions,  $Q_{(x, y_j)}$  are distributed if certain *condition* referred to stochastic factors is satisfied. The numbers are assigned to the indices in accordance with assignment shown in Fig. 2a (for clarity, only one example of the model nanowire at the initial position  $(x, y_{j=3})$  is depicted in Fig. 2b and reflecting of the  $C$  is not shown). The denotation,  $x'_l$  is used to indicate sites being nearest the  $y'_{jl}$  and so oriented in respect to the  $y'_{jl}$  as the site  $x$  is oriented in respect to  $y_j$ . In terms used for describing scheme of the hopping pairs (see, Fig. 1a), the denotation,  $(x'_l, y'_{jl})$  is used to indicate destination positions of the pairs. The rule of indexing presented here implies the equivalences,  $x'_{l=6} = x$  and  $y'_{j, l=6} = y_j$  (see the example for  $j = 3$  in Fig. 2b). The  $y'_{jl}$  can be covered for the  $A_i(T+1)$  if there is its neighbor site  $x'_l$  covered at

the stage  $T$ ,  $x'_l \in \{A_i(T) \cap V_{y'_{jl}}\}$  (here symbol  $\cap$  denotes taking common part of the sets).

The stochastic condition of the hopping-distribution of the  $Q_{(x, y_j)}$  from the  $S_x$  is assumed as requirement of obeying the inequality  $P_x(y_j) \geq r_x(y_j, i)$ . Here,  $r_x(y_j, i)$  is an element  $r_{x_k}(\xi_j, i)$  of the pseudo-random matrix  $\|r\|$  for  $x = x_k$ , where  $k = 1 \div N$ ,  $\xi_j = y_j$  for all  $j = 1 \div 6$ ,  $\xi_{j=7} = x_k$  and  $i = 1 \div M$ . The matrix  $\|r\|_{N \times 7 \times M}$  is computed by using a pseudorandom number generator (RANMAR [13] or, when noted, RANLUX [14, 15]) and independently of the stage  $T$  of the REP development (this is held also for other variants of the processes reported here). The  $P_x(y_j)$  is the probability assigned to a pair at the position  $(x, y_j)$ . The hopping-distribution of the  $Q_{(x, y_j)}$  which may result from activation of the pairs from positions  $(x, y_j)$  within  $S_x$  are independent events. Here, the value  $\sum_j P_x(y_j) \leq 1$  is equal to a probability  $P_s$  of occurring the signal transfers due to hopping-distribution of the  $Q_{(x, y_j)}$  from the  $S_x$  and the transfer will not take place due to stochastic factors with the probability  $(1 - P_s)$ .

#### C. Indirect transfer process REP-ITP

This variant of the REP corresponds to a process underlying evolution of a material system in which information about changing system features at a site can be distributed locally to engage more finite size elements into the transfer process.

One assumes that the signals  $C$  informing that a site  $z$  is covered,  $z \in A_i(T)$  are sent to all closest neighbors  $z_1$  of the  $z$  ( $z_1 \in V_z$ ) and each  $z_1$  redirects the signals. In this way, the  $C$  is enhanced to  $C_r$  that is delivered to all the  $x \in V_{z_1}$  (see Fig. 2c). This communication from the  $z$  to  $x$  is effective if the stochastic condition of the hopping-distribution of the  $Q_{(x, y_j)}$  is obeyed,  $P_x(y_j) \geq r_x(y_j, i)$  and there is the site  $x'_l \in \{A_i(T) \cap V_{y'_{jl}}\}$  so oriented in respect to  $y'_{jl}$  as the  $x$  is oriented in respect to  $y_j$  (see Section IIIB). In this case, the signal,  $Q_{(x, y_j)}$  is delivered to the  $y'_{jl}$  that is being covered,  $y'_{jl} \in A_i(T+1)$ . This scheme, identified as indirect transfer process (REP-ITP), allows exploring larger number of node configurations close to every site covered at a stage  $T$  while searching for pairs realizing transfers resulting in covering target sites at the stage  $T+1$ .

Note that  $x$  and  $z_1$  can be or can not be elements of  $A_i(T)$  and this ITP scheme allows also  $x$  coinciding with the  $z$  in the case of reflecting the signal by  $z_1$ . Thus local realization of the ITP can include the DTP as particular case. Eventually, it may happen that  $x \in A_i(T)$  when  $x \neq z$  or  $x \in A_i(T)$  because  $x = z$ . Both the cases correspond to contribution of the REP-DTP to the REP-ITP. Variant of the REP-ITP that allows only  $x \notin A_i(T)$  will be identified here as pure ITP (REP-ITP-P).



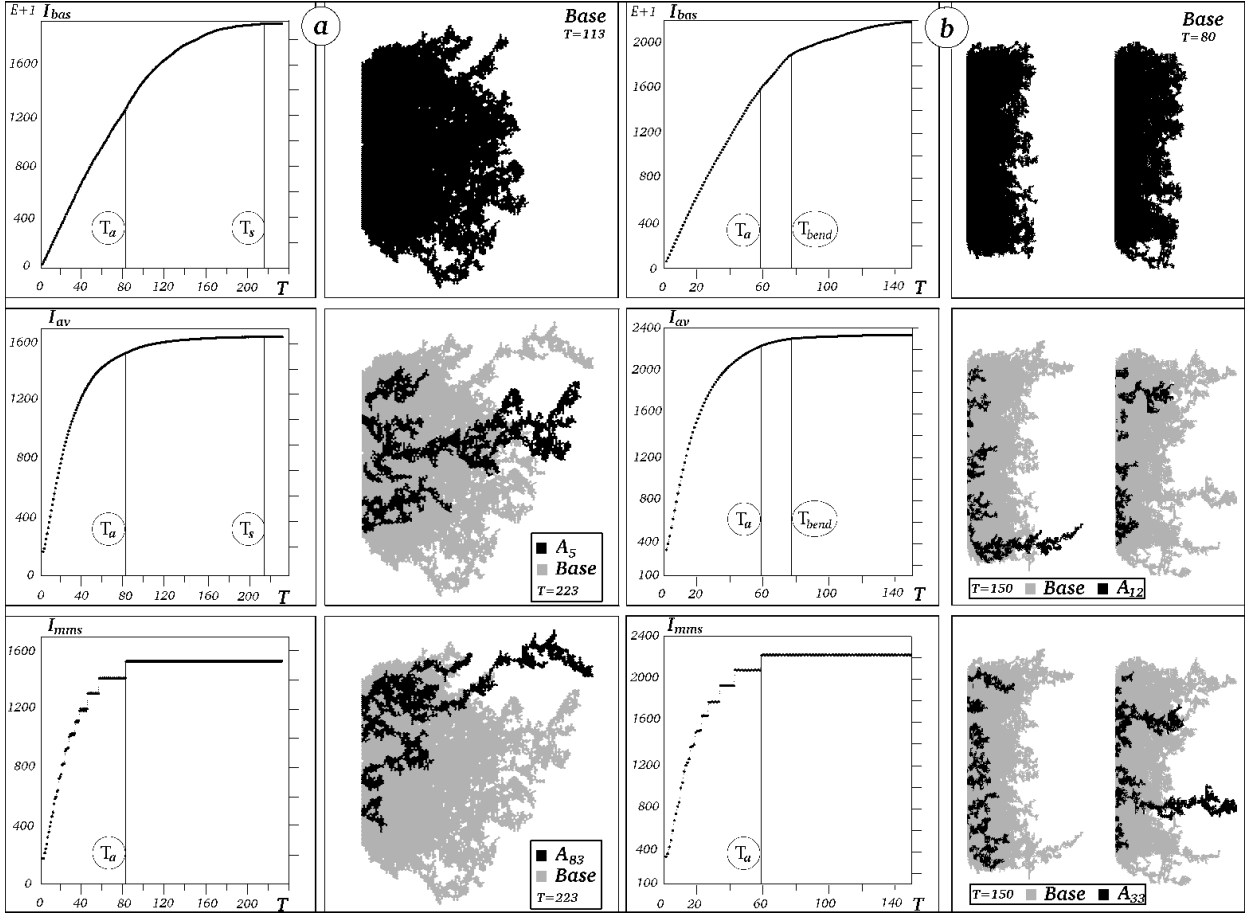


FIG. 3: Characteristics of the REP advancement shown for examples of REP-ITP representing two classes of evolution: (a) without a bend in  $I_{bas}(T)$ , here,  $\alpha = 0$ ,  $M = M_0 = 100$ ,  $P = 0.24$  (the sum  $E + 1$  means that the values shown should be multiplied by ten); (b) with the bend in  $I_{bas}(T)$ , here,  $\alpha = \frac{1}{3}$ ,  $M = M_0 = 100$ ,  $P = 0.1512$ . Two of six and two of five realizations developing yet at the very late stages are shown for examples of the classes (a) and (b), respectively. The realizations are depicted as dark patterns imposed on the brighter pattern of the base.

chains for the reliability purpose only, see Fig. 3b). The assignment of the  $P_j$  is assumed the same for both the REP variants, ITP and DTP, being investigated here. The value  $P$  parameterizes the model forcing factor affecting intensity of the expansion (limits to the  $P$  variation for the REP simulations being studied here are determined in Section VI A). The conditions assumed result in development of the areas covered within right half-plane from the IS (already at first stages of the REP, all the realizations evolve from the identical IS into actual finite random set, FRS defined in Section I). The resulting REP tends to stable bi-state represented by the MMS patterns that do not grow further (see Sections V A 1, V C). The schemes of local covering used to simulate the REP result in various forms of the covered area in the REP realizations,  $A_i$ . These can be sets of more or less dispersed rugged islands (see Fig. 2d, 3) and this diversity is specific to modeling the *finite-size effects*.

This specific feature of the REP realizations is revealed by comparison to a realization  $B_i$ , with  $i \leq M$ , of the spreading percolation (SPP) initiated from the same IS

and expanding within right half-plane (see Fig. 2d). The corresponding assignment of the site covering probabilities for the SPP is

$$P_1 = P_6 = 0, \quad P_7 \equiv 1, \quad P := P_2 = P_3 = P_4 = P_5 \leq 1. \quad (2)$$

In course of the SPP evolution, a site  $\xi \in S_x$ , with  $x \in B_i(T)$ , is covered for the  $B_i(T + 1)$  if  $P_x(\xi) \geq r_x(\xi, i)$  with  $\xi \in \{x, y_1, y_2, \dots, y_6\}$ . Thus, for the SPP, covering a site at a stage  $T$  implies its covering at  $T + 1$  that is not the case for the REP (see Eqs. (1) and (2)). Let us note that SPP is used here as simplest process, without modeling the F-SE and being comparable to the REP, which enables us to emphasize effects attributed to the F-SE modeling in the REP.

## B. Diversity parameters $N$ and $M$

For reliability of the systematic study of the REP, one requires comparing results of simulations obtained for ex-



tensive series of the parameter values  $P$ , in a spatial domain  $\chi = \{x_k, k = 1, 2, \dots, N\}$  with sufficiently large number  $N$  of elements (nodes) and for appropriate number  $M$  of the process realizations  $A_i$ ,  $i = 1, 2, \dots, M$ .

The number  $M$  of sets  $A_i$  constituting the ensemble (FRS) parameterizes degree to which diversity of the FRS manifests itself in features observed in sequence of the mean expected patterns,  $\int F(T)$  (i.e. in the sequence of MMS). The value,  $M_0$  limiting from below the number of realizations  $M$  being moderate assures that all the realizations have no site covered in common at any stage,  $T > 2$  of the random expansion process simulated. Number  $N \geq N_0 \approx 18000$  of sites constituting the space and  $M \geq M_0 \approx 100$  allow sufficient spatial-specific and ensemble-specific diversity modeled by respective computing the pseudo-random matrices  $\|r\|_{N \times 7 \times M}$ . The  $M$  different matrices having the size  $N \times 7$  and constituted by pseudo-random values are generated,  $r_{x_k}(\xi_j, i)$  with  $k = 1, 2, \dots, N$ ,  $\xi_j = y_j$  for  $j = 1, 2, \dots, 6$ ,  $\xi_7 = x_k$  and  $i = 1, 2, \dots, M$ . Assessment of the upper bound  $M_1$  to the  $M$  being moderate results from this investigation and is eventually presented in Section VIB3. The spatial domain,  $\chi$  should be sufficiently large to include each realization at latest required stage  $T_{mx}$  of the REP development,

$$\bigcup_x S_x \subset \chi \quad \forall x \in \text{base}[F(T)] = \bigcup_{i=1}^M A_i(T) \quad \forall T \leq T_{mx}. \quad (3)$$

The set,  $\text{base}[F(T)]$  will be called *base* of the FRS at the stage  $T$  of the REP development; the symbols  $\bigcup$  and  $\subset$  denote union and inclusion of sets whereas  $\forall$  is read "for all". Here, we have found that changes in number  $N$  only,  $N_0 \leq N \leq 16 \cdot N_0$  do not affect the simulation results remarkably.

### C. Lattice order projecting efficiency $\alpha$

The finite discrete space  $\chi$  is an example of a compact space that can be covered by finite number of open sets having a structural property in common, which is then inherited by whole the space (e.g. [16]. Here, this is the form of a regular hexagon. Extensive discussion of modelling the lattice order projecting efficiency has been presented by us previously [17]. There, we have revealed the ways of achieving isotropy of the symmetrical spreading on the hexagonal lattice, however, only one of them allows regulating *smoothly* the degree to which the lattice order is projected onto a process of the lattice covering. This way is followed here: One can select randomly a fraction  $\alpha$  of sites in  $\chi$ , for which covering all their six nearest neighbors is allowed. From the rest of sites, one selects randomly a half of them,  $(1 - \alpha)/2$  to allow covering only odd sites within their closest vicinities  $V_x$  (see Fig. 2a). For the remained half, one allows covering only even sites within the  $V_x$ . The symmetry and mutual situation of the odd and even triplets within the  $V_x$  result in

mutual neutralization of their contributions to the inheritance effect. This can be observed for clusters constituted by sufficient number of sites covered. Eventually, the  $\alpha$ ,  $0 \leq \alpha \leq 1$ , parameterizes efficiency of projecting the order of regular hexagonal array onto patterns resulting from the REP development.

## V. CHARACTERISTICS OF THE REP DEVELOPMENT

### A. Characteristics of the process advancement

#### 1. Reference to finiteness and discreteness

After few initial stages, advancement in the REP development (either ITP or DTP) is characterized by monotonic growth in the average number of nodes covered in a realization,

$$I_{av}(T) = \frac{1}{M} \sum_{i=1}^M I_i(T), \quad (4)$$

with  $I_i(T) = \mu\{A_i(T)\}$ , and in the number of nodes constituting the base,

$$I_{bas}(T) = \mu\{\text{bas}[F(T)]\} \quad (5)$$

as well as by stepwise growth in the number of nodes of the MMS representation,

$$I_{mms}(T) = \mu\left\{\int F(T)\right\}. \quad (6)$$

Here,  $\mu\{\cdot\}$  denotes the number of elements of the finite set  $\{\cdot\}$  (see previous Sections for other denotations). The REP finishes at a stage  $T_s$ , until which all the  $M$  realizations have finished their development (see Fig. 3a). A stage  $T_a$ , since which  $I_{mms}(T)$  does not grow further, identifies beginning of the REP *advancement* period. Realizations  $A_i(T)$ ,  $i = 1, 2, \dots, M$  can finish their development at various stages  $T \leq T_s$ . This variety of the realization evolutions results in  $I_{bas}(T)$  growing much stronger than  $I_{av}(T)$  for  $T > T_a$  (see Fig. 3). In virtue of very small reductions in realizations in all REP simulations reported here, approaching the  $T_s$  can be indicated by the  $I_{bas}(T)$  and  $I_{av}(T)$  becoming constant.

One may observe specific distribution,  $I_{bas}(T)$  in the beginning of the period following the  $T_a$  which corresponds to forms of not overlapping parts of few growing realizations. For example, a bend in the  $I_{bas}(T)$ , which can be observed around a stage  $T_{bend}$  occurring close to the  $T_a$ , corresponds to change in form of increments in the base from rather uniform front like advancement to few narrow separated tongues preserving direction of the expansion (see Fig. 3b).

We have found that smooth transition of the  $I_{av}(T)$ , from strong growth to very weak increments, indicates

finishing of the evolution for major part of the realizations. These realizations,  $A_i(T)$  finish their development rather abruptly within a period identified by the series of few stages which can be indicated conventionally by a central stage,  $T_{bend}(i)$  of this period. This is indicated by a bend in the distribution  $I_i(T)$ . The  $I_i(T)$  grows strongly until the bend and becomes constant for the following stages. Diversification of the values  $T_{bend}(i)$  within the set corresponding to the  $M$  realizations and lack of the bend in  $I_i(T)$  for a number of them result in the smooth distribution of the  $I_{av}(T)$ .

## 2. Specific effect of discreteness - steps in $I_{mms}(T)$

The growing length of steps in the  $I_{mms}(T)$  evidences approaching the  $T_a$  (see Fig. 3). We explain appearance of the steps in the  $I_{mms}(T)$  with reference to the method of determining the MMS (see Appendix ).

At a stage  $T$ , one determines the  $I_{av}(T)$  and pairs of sets,  $\Phi_i(T)$  or  $\phi_i(T)$  constituted by such covered sites that a number of  $k \geq i$  or  $k > i$  realizations have them in common, respectively. For the numerical criterion  $h = i/M$  used to determine the MMS, one selects such value  $i$  that with this  $i$  the inequalities  $\mu\{\phi_i(T)\} \leq I_{av}(T) \leq \mu\{\Phi_i(T)\}$  are obeyed. A number of such covered sites that more than  $i = const$  realizations have them in common can grow with  $T$  for certain period. Therefore, the values  $\mu\{\Phi_i(T)\}$  and  $\mu\{\phi_i(T)\}$  can also grow with the  $i = const$  to satisfy the noted inequalities when  $I_{av}(T)$  increases with  $T$ . At certain stage of the following evolution, increment in contribution to  $I_{av}$  from less overlapping branches of the realizations requires selecting smaller value  $i$  to obey these inequalities. This change in the  $i$  causes jump of increment in the  $I_{mms}$  as stronger as larger is the contribution from not overlapping branches of the realizations. The period with  $i = const$  is as longer as slower is growth in  $I_{av}$  and as slower is growth in contribution to the increment in  $I_{av}$  from dispersed in space, less overlapping branches of the realizations. This explains growth in length of the subsequent periods corresponding to subsequent values  $i = const$ , respectively. In virtue of the effects indicated by the steps in  $I_{mms}(T)$ , we will call the corresponding time intervals the *accumulation periods*.

Thus appearance of the steps results from discreteness of the realization ensemble and their significance can be attributed to the remarkable share which not overlapping extended branches of the realizations have to the  $I_{av}$  in the REP with the moderate  $M$ .

At earlier stages of the evolution, influence of the various factors onto the  $I_{mms}(T)$  is more complex and indicates significant contribution from overlapping branches of the realizations.

## B. Structural characteristics

Characteristics of *local* clustering which have been collected within whole the space  $\chi$  provide information about the pattern accomplished within the  $\chi$  at a stage  $T$ . For that pattern, one may define a probability  $\mathcal{P}_n$  of finding a cluster constituted by exactly  $n$  sites covered within closest neighborhood  $S_x$  of a site  $x \in \chi$ . We express it as  $\mathcal{P}_n = \mathcal{R}_n/\mathcal{N}_b$  with  $\mathcal{N}_b$  being number of sites within the smallest rectangle circumscribing the  $base[F]$  and  $\mathcal{R}_n$  being number of these sites  $x$  with the  $S_x$  containing not less than one cluster constituted by exactly  $n$  sites covered ( $2 \leq n \leq 7$ ); note that using the form of a rectangle is just a convenient choice. It is easy to see that occurrence of the  $n$ -site cluster within  $S_x$  does not allow occurrence of a separate cluster constituted by different number,  $n_1 \neq n$  and  $n_1 \geq 2$ , of sites within this  $S_x$ .

Let us imagine a free gliding window  $S$  congruent with  $S_x$  which appears at a site  $x$  if the  $S_x$  coincides with this window (see Fig. 2a). We follow an approach known from the information theory [18] and consider the window  $S$  as an information channel. A pattern that can be observed within the  $S$  can be considered as the information carrier passing through this channel. Distinct clusters composed of certain number  $n$  of sites are independently transferred by the carrier through this channel while the free window  $S$  appears once at each site within the smallest rectangle circumscribing the  $base[F]$ . Accordingly, one may consider the value,

$$H_n = -\mathcal{P}_n \cdot \ln \mathcal{P}_n \quad (7)$$

as contribution from passing the  $n$ -site cluster to mean expected amount of information that can be transferred by the carrier through the channel  $S$ . The sum,  $H = -\sum_{n=2}^7 H_n$  is used here as reference scale for the  $H_n$ . Distributions of these relationships against the  $T$ , not just their values at  $T$  fixed, characterize the evolution of the MMS or  $A_i$  realization patterns. They are called here, for brevity, the *entropic characteristics*. We denote these values determined for the MMS pattern as,  $H_{mms}$ ,  $(H_n)_{mms}$ ,  $(H_n/H)_{mms}$ . The values,  $H_i$ ,  $(H_n)_i$ ,  $(H_n/H)_i$  are determined for a distinct realization  $A_i$  whereas  $H_{av}$ ,  $(H_n)_{av}$ ,  $(H_n/H)_{av}$  denote mathematical expectations of the entropic characteristics determined for every realization of the FRS.

## C. Features of MMS evolution

### 1. Structural bi-state

Accomplishment of the structural bi-state in course of a number of initial stages of the REP development is specific feature of modeling the finite-size effects. Appearance of the bi-state in the MMS development is well illustrated by the graphs of the  $(H_n/H)_{mms}$  (see

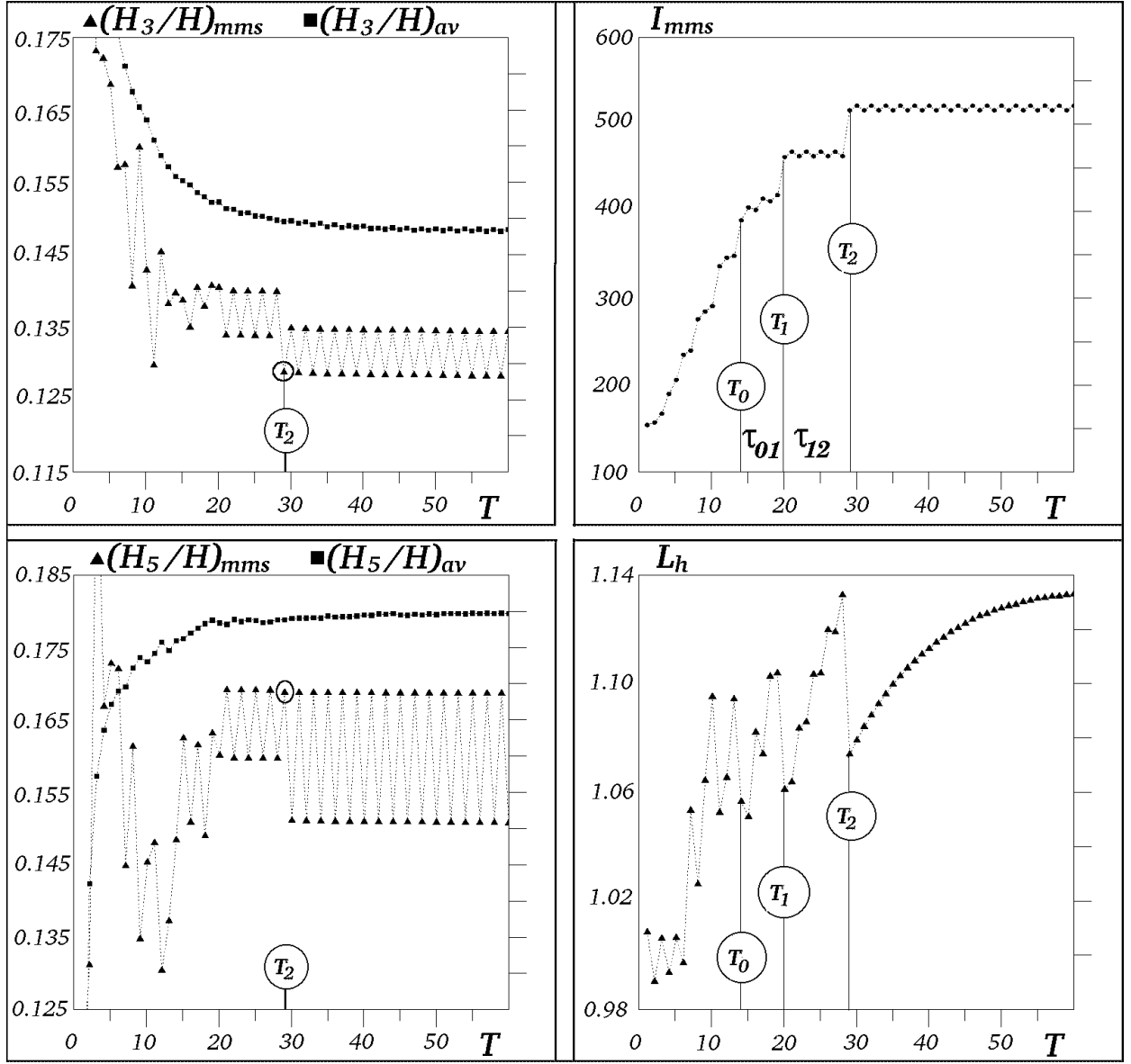


FIG. 4: Characteristics of structural bi-state stabilization in the MMS development for example of the REP-ITP with  $\alpha = \frac{1}{3}$ ,  $M = M_0 = 100$ ,  $P = 0.1311$ . The same value  $T_2$  is identified in all graphs  $(H_n/H)_{mms}(T)$  with  $2 \leq n \leq 7$  (here, only the examples are shown).

Fig. 4). Saw-shaped distribution of the  $(H_n/H)_{mms}$  against  $T$  depicts these values at subsequent stages  $(T, T+1)$  as corresponding to states of the bi-state. Situation of the points representing the subsequent pairs,  $\{(H_n/H)_{mms}(T), (H_n/H)_{mms}(T+1)\}$  on parallel lines for an accumulation period detects structural bi-state stability of the MMS development within this period. Then, a pair of neighbor stages computed,  $(T, T+1)$  corresponds to a single physical stage when the system may be in one as well as in the other structural state. Result of this type has been reported by us previously [9] as the one attributed to modeling the finite-size effects and, then, its relevance to available experimental observations has been noted.

The REP simulated accordingly to the REP-ITP and REP-DTP reveals features of the bi-state stabilization. Let us recall that patterns of covered sites, which are being accomplished within whole the spatial domain in course of the REP-ITP, may be considered as resulting from processes of covering the sites according to both the schemes, REP-DTP and REP-ITP-P (see Section IIIC). However, the REP simulations performed accordingly to the REP-ITP-P scheme only, resulted in appearance of the bi-state with no features of its stabilization. This shows that sufficient contribution from the REP-DTP to the REP-ITP is the necessary condition of the bi-state stabilization for the REP-ITP. This condition is satisfied for all the REP-ITP simulations reported

here (effect of the contribution which REP-DTP has to REP-ITP is elucidated in Section VIB 2).

### 2. Bi-state stabilization events, $T_0, T_1, T_2$

Appearance of the bi-state stability at the end  $T_e$  of certain accumulation period is identified if this effect encompasses the computed sequence from  $(T_e + 1 - 2 \cdot t)$  to the  $T_e$ , with  $t \geq 2$ , for the  $(H_n/H)_{mms}(T)$  for all  $n$ ,  $2 \leq n \leq 7$ . The bi-state stability accomplished is preserved for all the following accumulation periods. One may observe such accumulation period that its end indicated by the  $T_e$  is the first computed stage in course of the evolution, for which the conditions just mentioned are obeyed. Then, the stage  $(T_e + 1)$  is denoted as  $T_2$  and corresponds to the first jump from one structurally stable bi-state to other such bi-state (see Fig. 4). This corresponds to a jump in the  $I_{mms}(T)$  between corresponding neighbor steps, however, the  $I_{mms}(T)$  cannot replace the  $(H_n/H)_{mms}(T)$  in unambiguous detecting the  $T_2$ . The accumulation period preceding the  $T_2$  begins at the stage denoted as  $T_1$  whereas the one preceding this begins at the stage denoted as  $T_0$ . Having given the  $T_2$ , both the  $T_1$  and  $T_0$  can be easily detected as stages corresponding to local minima in distribution of a helping characteristic  $L_h(T) = 1 + (H_{av} - H_{mms})/H_{av}$  (see Fig. 4) or, for higher values of  $P$ , as instants of jumps between steps in the  $I_{mms}(T)$ .

The distributions,  $(H_n/H)_i(T)$  with  $1 \leq i \leq M$ , reveal that  $T_0$  or  $T_1$  is within a short sequence of the stages since which the realizations can start accomplishing the bi-state not stable yet or can accomplish stable structural bi-state, respectively (see Fig. 5); hereafter we will use also the phrase *becoming bi-stable* as abbreviation to *accomplishing the stable bi-state*. Significant part of realizations becomes bi-stable until the  $T_2$ , however, a number of them becomes bi-stable very late after the  $T_2$  and they begin accomplishing the bi-state close to the  $T_1$ .

Eventually, one may consider the triplet,  $T_2, T_1, T_0$  as values characterizing evolution of the MMS pattern in the

REP. Their distributions against  $P$  can reveal possible regular changes in these evolutions with varying  $P$ .

### 3. Characteristic increments in the MMS development

Sets being increments in the  $\int F(T)$  for the accumulation period or at the jump between these periods are to be determined for the same state of the bi-state (see Fig. 6). These sets are denoted as  $\delta \int F$  and identified by the pair of indices  $l, k$  or  $lk$  for the respective accumulation period whereas index  $T_j$  is used to indicate sets being increments at a jump at the  $T_j$ . Accordingly, the pairs 01 or 12 indicate sets being increments in the  $\int F(T)$  for the accumulation periods, from  $T_0$  to  $T_1$  or from  $T_1$  to  $T_2$ , respectively. The accumulation periods,  $\tau_{l,k}$  and instances of the jump events  $T_j$  are calculated for each state of the bi-state. We calculate length of the accumulation period between simulated stages for  $l \in \{0, 1\}$  and  $k = l + 1$  as,  $\tau_{l,k} = t_k - T_l + 1$ , with  $t_k = T_k - 1$  or  $t_k = T_k - 2$ , so that  $t_k$  and  $T_l$  are both odd or they both are even. One considers increments  $\delta \int F_{l,k}$  corresponding to the  $\tau_{l,k}$ : between  $T_l$  and  $t_k$  for one state and between  $T_l + 1$  and  $t_{k,A}$  for the other, with  $t_{k,A} = t_k - 1$  if  $t_k = T_k - 1$  or  $t_{k,A} = t_k + 1$  if  $t_k = T_k - 2$ . The increments  $\delta \int F_{l,k}$  are determined accordingly to Eq. (8). The nonnull reductions,  $\delta \int F_{k,l}$  determined in accordance with Eq. (9) may accompany these increments. Changes in forms of these increments and reductions with varying the  $M$ ,  $\alpha$  and  $P$  are considered in Section VIB 3. Increments in  $\int F$  corresponding to a state of the bi-state at the jump in MMS growth at  $T_j$  are sets of sites scattered throughout whole the  $\int F$  and they are not accompanied by a reduction in the MMS. They are denoted as  $\delta \int F_{T_j}$  and determined accordingly to Eq. (10). Differences  $\Delta \int F(T, T + 1)$  between MMS corresponding to the two states of the bi-state are given by Eq. (11) and they have also the form of a set of covered sites dispersed throughout the  $\int F$ . All the sets just noted are given by the following relationships,

$$\delta \int F_{l,k} \in \left\{ \int F(t_k) \setminus \int F(T_l), \int F(t_{k,A}) \setminus \int F(T_l + 1) \right\}, \quad (8)$$

$$\delta \int F_{k,l} \in \left\{ \int F(T_l) \setminus \int F(t_k), \int F(T_l + 1) \setminus \int F(t_{k,A}) \right\}, \quad (9)$$

$$\delta \int F_{T_j} \in \left\{ \int F(T_j) \setminus \int F(T_j - 2), \int F(T_j + 1) \setminus \int F(T_j - 1) \right\}, \quad (10)$$

$$\Delta \int F(T, T + 1) = \left\{ \int F(T) \setminus \int F(T + 1), \int F(T + 1) \setminus \int F(T) \right\}, \quad (11)$$

(here,  $A \setminus B$  denotes elements of a set  $A$  which are not elements of the set  $B$ ). The form of increment in the

MMS depicted in Fig. 6 for example of the  $\delta \int F_{T_2}$  as well

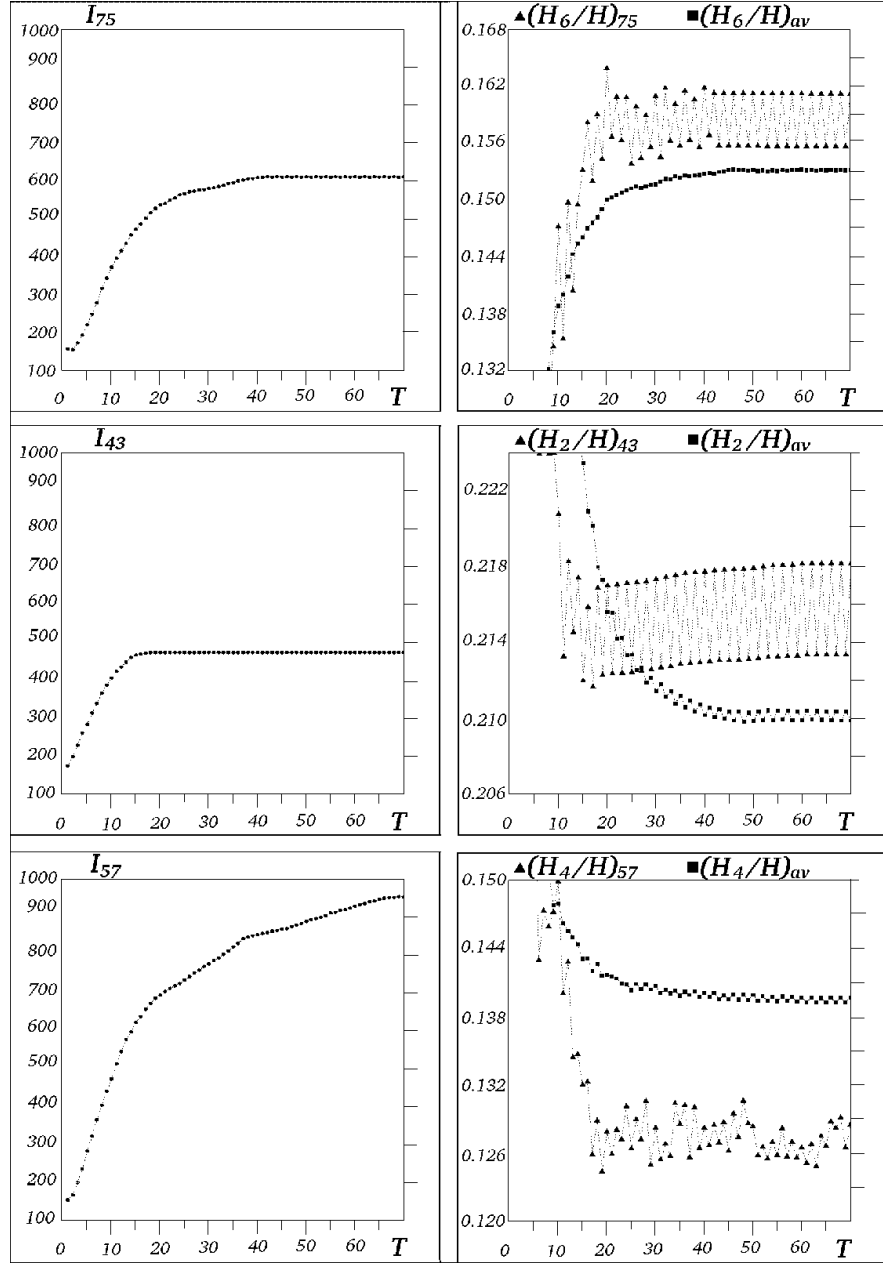


FIG. 5: Examples of characteristics representing three recognized classes of originating the structural bi-state and its stabilization in a realization development. For this example of the REP-ITP with  $\alpha = \frac{1}{3}$ ,  $M = M_0 = 100$ ,  $P = 0.1311$  (then,  $T_0 = 14$ ,  $T_1 = 20$ ,  $T_2 = 29$ ), of about 35% of the realizations  $A_i(T)$  have appeared in stable structural bi-state before the stage  $T = T_2$ . Observe that appearance of the bi-state close to  $T_0 = 14$ , at  $T = 15 > T_0$  ( $i = 75$ ) or at  $T = 13 < T_0$  ( $i = 43$ ) corresponds to its stabilization and becoming the  $I_i(T) = \text{const}$  at stages  $T = 42 > T_2$  ( $i = 75$ ) or  $T = 18 < T_1$  ( $i = 43$ ). Here, later origination of the bi-state in development of the realization  $i = 57$  corresponds to absence of the stabilization in the  $A_{57}(T)$  before  $T = 70 \gg T_2$ .

as  $\Delta \int F(T, T+1)$  will be identified as *scattered increment*.

Sequences of patterns representing evolution of distinct realizations  $A_i(T)$  reveal nature of accomplishing the bi-state and thus elucidate emerging the characteristic forms of the increments in MMS in course of the REP development. Example of such sequence is presented in the array of patterns shown for  $A_{57}$  in Fig. 6. Specifically developed form of the realization within its central

region, distanced from the fronts, results from accomplishment of the bi-state. No bias from this specific feature in evolution of a realization has been observed either for REP-DTP or REP-ITP simulated here.

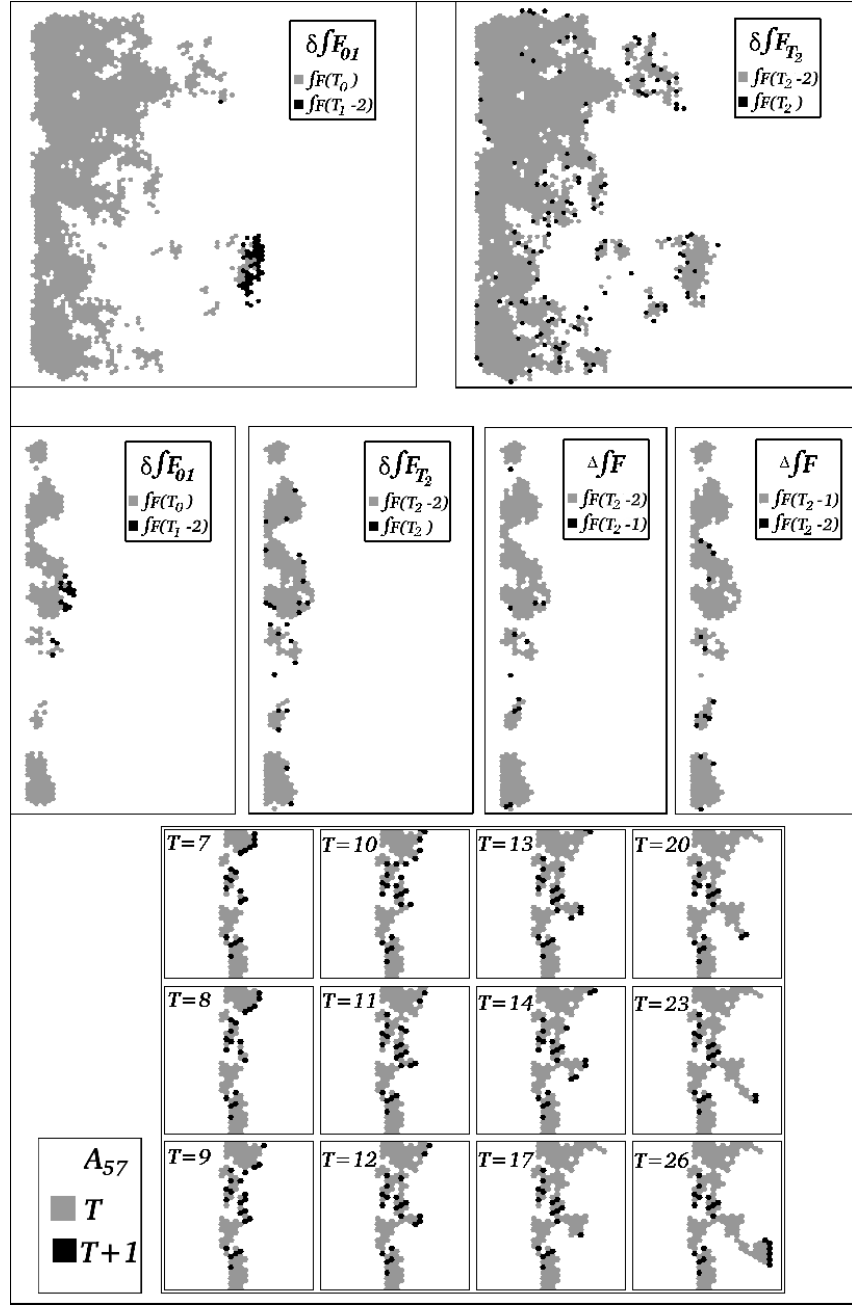


FIG. 6: Pairs of MMS patterns imposed one on the other to show characteristic increments in the MMS in course of the REP evolution. For example of a region in one REP realization  $A_{57}$ , the pairs of imposed patterns are shown to reveal appearance of the bi-state. In all figures, bright pattern is imposed on the dark one. All figures have been obtained by simulating the REP-ITP with  $\alpha = \frac{1}{3}$ ,  $M = M_0 = 100$ . The top pair of patterns results from the simulation with high  $P = 0.18$  (then,  $T_0 = 82$ ,  $T_1 = 92$ ,  $T_2 = 101$ ) whereas all other figures with low  $P = 0.1311$  (then,  $T_0 = 14$ ,  $T_1 = 20$ ,  $T_2 = 29$ ).

## VI. RESULTS AND DISCUSSION

One searches for regularities in changes of the MMS evolution patterns  $\int F(T)$  with varying the process parameters  $P$ ,  $\alpha$ ,  $M$ . Results of the previous section suggest that distributions,  $T_0(P)$ ,  $T_1(P)$ ,  $T_2(P)$ ,  $\tau_{01}(P)$ ,  $\tau_{12}(P)$  with  $P$  varying within an interval when  $\alpha$ ,  $M$  are kept constant may reveal such regularities. The

corresponding increments  $\delta \int F_{T_j}$ ,  $\delta \int F_{01}$ ,  $\delta \int F_{12}$  associate the changes in the characteristics with features of the MMS evolution patterns. Accordingly, one investigates these characteristic distributions with fixed parameters  $\alpha \in \{0, \frac{1}{3}, 1\}$  and  $M = M_0 = 100$ . Dependence of the  $\int F(T)$  on the number of realizations  $M$  is investigated with the purpose to estimate the upper limit  $M_1$  to the values  $M$  being moderate.

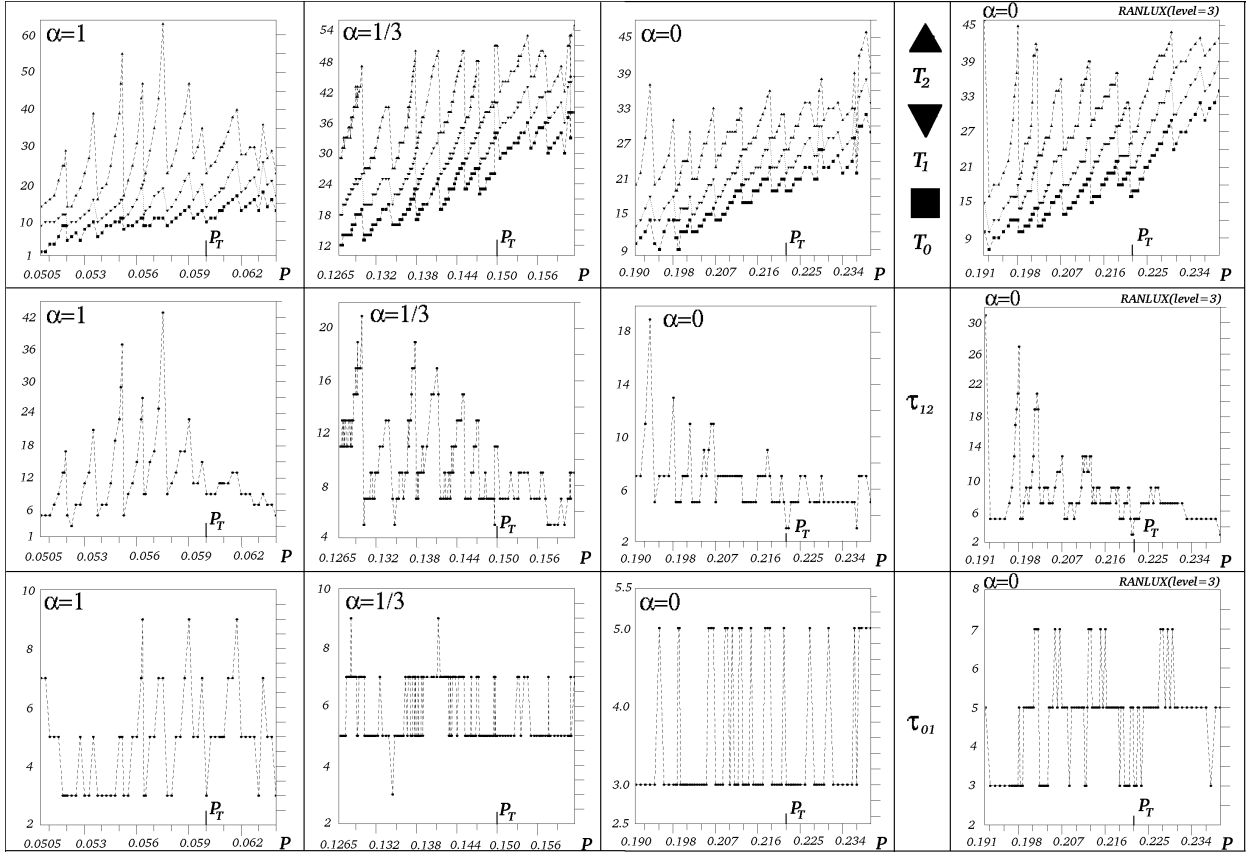


FIG. 7: Regular variations of the MMS bi-state stabilization event characteristics with  $P$  and  $\alpha$ . All the REP-ITP simulations have been done with  $M = M_0$ , the same pseudo random matrix,  $\|r\|_{N_0 \times 7 \times M_0}$  and space of  $N = N_0$  sites. The same pseudo random number generator RANMAR has been employed to compute this matrix and to satisfy the condition,  $\alpha < 1$ . Only the control distributions shown in the column most to right have been obtained by using the more advanced generator RANLUX (with luxury level=3).

#### A. Distributions $T_j(P)$ , $\tau_{01}(P)$ , $\tau_{12}(P)$

The three sets of distributions  $T_j(P)$ ,  $\tau_{12}(P)$ ,  $\tau_{01}(P)$  have been obtained from the series of REP-ITP simulations with  $\alpha \in \{1, \frac{1}{3}, 0\}$ ,  $M = M_0$ , in the same space  $\chi$  ( $N_0 \approx 18000$  nodes) and by employing the same matrix  $\|r\|_{N_0 \times 7 \times M_0}$  of pseudo-random numbers. The generator RANMAR [13] has been employed to compute the matrix  $\|r\|_{N_0 \times 7 \times M_0}$  and to satisfy condition of the lattice order projecting efficiency  $\alpha < 1$  (see Section IV C). Three triplets of graphs depicting the distributions  $T_j(P)$ ,  $\tau_{12}(P)$ ,  $\tau_{01}(P)$  with  $\alpha \in \{1, \frac{1}{3}, 0\}$  are presented in Fig. 7. With the purpose to recognize an effect of using a particular pseudo-random number generator, they are compared to results of the REP-ITP simulation series repeated with employing the more advanced generator RANLUX(luxury level=3) [14, 15] instead of using RANMAR to compute the  $\|r\|_{N_0 \times 7 \times M_0}$  and to satisfy the requirement  $\alpha = 0$ . This comparison reveals only quantitative differences that appear to have no effect onto inferences about qualitative features of certain regularities observed in the distributions. Therefore, the simpler

generator RANMAR has been considered as sufficient to obtain reliable results for the purpose of this research.

The interval of the values  $P$  used to perform series of the REP-ITP simulations has been selected specifically for each value of the  $\alpha \in \{1, \frac{1}{3}, 0\}$ . The lower limit of the  $P$  variations has been selected so as to obtain the REP-ITP evolutions revealing clearly occurrence of all the three instants  $T_0$ ,  $T_1$ ,  $T_2$ . The upper limit has been assumed with the help of the  $\tau_{12}(P)$ . One may observe qualitative change in variation of the  $\tau_{12}$  with growing  $P$  starting from certain threshold value  $P = P_T(\alpha)$ . For  $P > P_T$ , the value  $\tau_{12}(P)$  appears to vary more regular and within fixed interval (see Fig. 7). This enables us to estimate,  $P_T(\alpha = 0) \approx 0.222$  (for RANMAR and RANLUX),  $P_T(\alpha = \frac{1}{3}) \approx 0.150$ ,  $P_T(\alpha = 1) \approx 0.060$ , that correspond to the beginning of certain interval  $[P_a, P_b]$  within which the  $T_j(P)$  is growing (see Fig. 7 and Fig. 8; appearance of such intervals is elucidated in next Section VIB 1). The  $P_T(\alpha)$  appears to be indicated also by specific distributions  $T_j(P)$  within two neighbor subintervals,  $[P_a, P_b]$  situated just to left of the  $P_T$  and within the subinterval just to right of the  $P_T$ . Eventually, the upper limit of the  $P$  has been assumed so as to encompass not

less than two subintervals  $[P_a, P_b]$  following the  $P_T(\alpha)$ . A number of test simulations performed accordingly to the REP-ITP scheme with the  $P$  being substantially higher than the limits selected seem to corroborate reliability of using the  $P_T(\alpha)$  to assess scope of the  $P$  abscissa for this investigation.

Form of the graph  $T_j(P)$  resembling quasi-periodical distribution as well as occurrence of the  $P_T(\alpha)$  are specific to the REP-ITP and have not been observed for REP-DTP simulation series. The distribution,  $T_j(P)$  is much less regular for the REP-DTP simulated with the  $M \approx M_0$  (see Fig. 8) and much more complex for the REP-DTP series computed with high values of the  $M$ .

## B. Structural pattern of changes in REP series

### 1. Appearance of intervals $[P_a, P_b]$

Interpretation of the distributions  $T_j(P)$  requires comparing the corresponding realizations,  $A_i(T)$  with the same  $i < M$ , in the REP simulation series of the same type, performed with close values  $P$  constituting the growing series and with other parameters being the same for these simulations.

One can observe that there are intervals of the value  $P$  within which a small increment in  $P$  may result in covering some sites being incipient elements of substantial branches developing in some realizations. In virtue of the  $M$  being moderate, those branches can postpone occurrence of the  $T_2$  (see also Sections V A 2, V C 2). Further growth in  $P$  may result in covering more sites constituting the incipient elements of the branches in larger number of realizations. Evolutions of the corresponding realizations obtained with close values of  $P$  and for the respective accumulation periods reveal growth of the spots covered, increment in number of those spots and, eventually, spatial uniformization of their arrangement (see Fig. 8). Then, one may observe growth in number of covered spots distributed along an interval being parallel to the initial chain (see the example of  $A_{11}$  in Fig. 8) or expansion of the localized tongues also in this direction (see the example of  $A_{73}$  in Fig. 8). The spatial uniformization of the realizations appears to be sufficient for stabilization of the bi-state at an earlier stage of the evolution if  $P$  becomes slightly greater than certain value  $P^*$  (the  $P^*$  appears as right-hand end of the interval alluded to previously; the  $P$  just mentioned as being slightly greater than the  $P^*$  is denoted as  $P_{\oplus}^*$ ). This earlier stage appears closer to the  $T_1$  detected in the evolution performed with  $P$  being slightly smaller than  $P^*$  (this value of  $P$  is denoted by  $P_{\ominus}^*$ ). Thus the inequality,  $T_2(P_{\ominus}^*) > T_2(P_{\oplus}^*)$  is obeyed. Nature of the changes just revealed explains repetition of the scenario for the REP evolutions with the  $P$  growing further and thus appearance of subsequent intervals  $[P_a^*, P_b^*]$  (they are denoted also simpler as  $[P_a, P_b]$ ).

### 2. Synchronisation effect of covering sites in REP-ITP

The distributions  $T_j(P)$  obtained from the series of the REP-ITP simulations reveal variation resembling the quasi-periodical one and  $T_2(P)$  grows rather monotonically within the intervals  $[P_a, P_b]$  (see Fig. 7 and Fig. 8). This is accompanied by systematic dependence of the average length  $\mathcal{L}_P$  of intervals  $[P_a, P_b]$  on the  $\alpha$ :  $\mathcal{L}_P(\alpha)/\mathcal{L}_P(\alpha=1) \approx 3-2\alpha$ . Evolutions of realizations in the REP-ITP series simulated with the series of  $P$  growing within the  $[P_a, P_b]$  toward the  $P_b$  ( $P \rightarrow P_b$ ) result in covering larger number of sites dispersed in the space. Then, more stages is required to accomplish sufficiently dense sets of the sites covered in the realizations to enable sufficient contribution from the REP-DTP to REP-ITP for stabilization of the bi-state (this contribution has been explained in Section V C 1). Further growth of the  $P$ , until  $P_{b\oplus}$  is reached, results in denser covering the area in realizations  $A_i(T)$  so that contribution from the REP-DTP to REP-ITP becomes more substantial and the stabilization occurs earlier. This may be interpreted as result of *synchronization* between site covering accordingly to the REP-ITP-P and REP-DTP schemes considered as components of the REP-ITP scheme.

One may note following factors contributing to the regularity of the distributions  $T_j(P)$ . The REP-ITP differs from the REP-DTP in exploring the larger number of site configurations within neighborhoods of sites covered at a stage  $T$  while searching for pairs realizing transfers resulting in covering target sites at the stage  $T+1$  (see Section III C and Fig. 2c). This results in comparable contribution of all the realizations  $\{A_i\}_{i=1 \div M}$  to the MMS in the REP-ITP simulations. Preserving the symmetry in the arrangement of the odd or even sites whose covering is allowed within vicinities  $V_x$  with  $\alpha < 1$  (see Section IV C and Ref. [17]) facilitates more uniform covering the space in realizations  $\{A_i\}_{i=1 \div M}$  and, eventually, appears to improve harmony between the distributions  $T_2(P)$ ,  $T_1(P)$  within the intervals  $[P_a, P_b]$  (see Fig. 9).

### 3. Variations of MMS evolution patterns with $P$ , $\alpha$ , $M$

Dependence of the increments,  $\delta \int F_{01}$ ,  $\delta \int F_{12}$  on the simulation parameters  $P$ ,  $\alpha$  with  $M = M_0$  is presented for the REP-ITP in Table I. Note that there are no increments for the accumulation periods following the  $\tau_{12}$  if  $\delta \int F_{12}$  vanishes. Occurrence of reductions,  $\delta \int F_{10}$  and  $\delta \int F_{21}$  accompanying increments,  $\delta \int F_{01}$  and  $\delta \int F_{12}$  in the MMS for the accumulation periods  $\tau_{01}$ ,  $\tau_{12}$  as well as characteristic differences between those increments (reductions) in the REP-ITP evolutions, with  $P \rightarrow P_{a\oplus}$  and  $P \rightarrow P_{b\ominus}$  for all  $[P_a, P_b]$ , are specific features of the REP-ITP simulated with higher values of the  $\alpha$ ; the reductions have not been observed for REP-ITP with small values of the  $\alpha$  and for the REP-DTP (see Tables I, II). Appearance of harmony between the distribu-



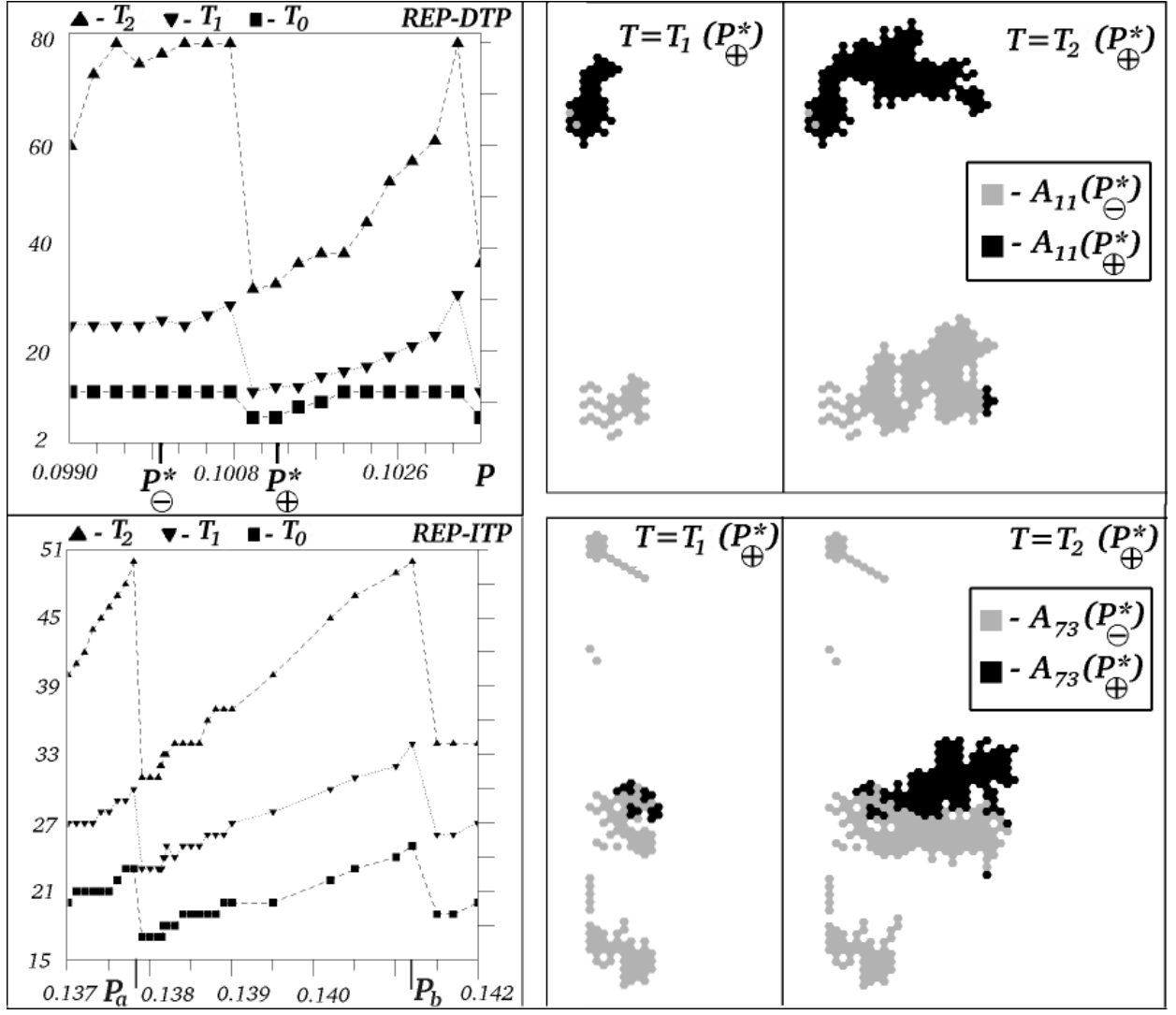


FIG. 8: Spatial uniformization of contributions to the MMS from realizations of the REP simulated with series of the  $P$ . This uniformization, which corresponds to appearance of the critical value  $P^*$ , is shown for example of the REP-DTP series with  $M = 104 \approx M_0$ ,  $\alpha = 1$  and growing  $P$  (here,  $P_{\ominus}^* = 0.10000 < P^* < P_{\oplus}^* = 0.10125$ ). The figures depict bright pattern imposed on the black one. Regular character of distributions  $T_j(P)$  within interval of  $P$  between subsequent critical values,  $P_a$ ,  $P_b$  is specific to the REP-ITP; this is shown for example obtained with  $\alpha = \frac{1}{3}$ ,  $M = M_0 = 100$ .

tions  $T_0(M)$ ,  $T_1(M)$ ,  $T_2(M)$  indicates certain threshold value  $M_{\tau}$  (see Fig. 10). The REP-ITP simulation series done with  $M$  slightly smaller or slightly greater than  $M_{\tau} \approx 160$  result in the specifically different increments  $\delta \int F_{01}$ . Similar effect, concerning however the  $\delta \int F_{12}$ , has been observed for example of the REP-DTP series (see Table II). Let us recall that in course of REP evolution simulated with  $M \approx M_0$ , the increments  $\delta \int F_{T_j}$  appear in form of a number of few site clusters and single sites scattered throughout whole the  $\int F$ . On the other hand, the corresponding spreading percolation SPP (see Section IV A), being the simplest process without modeling the finite-size effects which can be compared to the REP, results only in dispersed sedimentation-type increments in the MMS that occur only at jumps between steps in

the  $I_{mms}(T)$  (see Fig. 10). These increments can be compared to the  $\delta \int F_{T_j}$  that correspond to jumps in the  $I_{mms}(T)$  appearing in course of the REP evolution. The difference revealed by this comparison can be attributed to accomplishment of the bi-state that is peculiar to modeling the finite-size effects in accordance with the REP covering scheme. We have, however, observed that the REP-ITP simulated with the sufficiently high  $M$  results in the  $\delta \int F_{T_j}$  that, with growing  $M$ , are being reduced to the forms of dispersed sedimentation-type increments resembling, to some extent, the increments resulting from the SPP (see Fig. 10). This resemblance does not mean reducing the REP to SPP or vanishing the F-SE; the bi-state and its stabilization events at  $T_j$  are further present. Only effects attributed to *discreteness* of the informa-

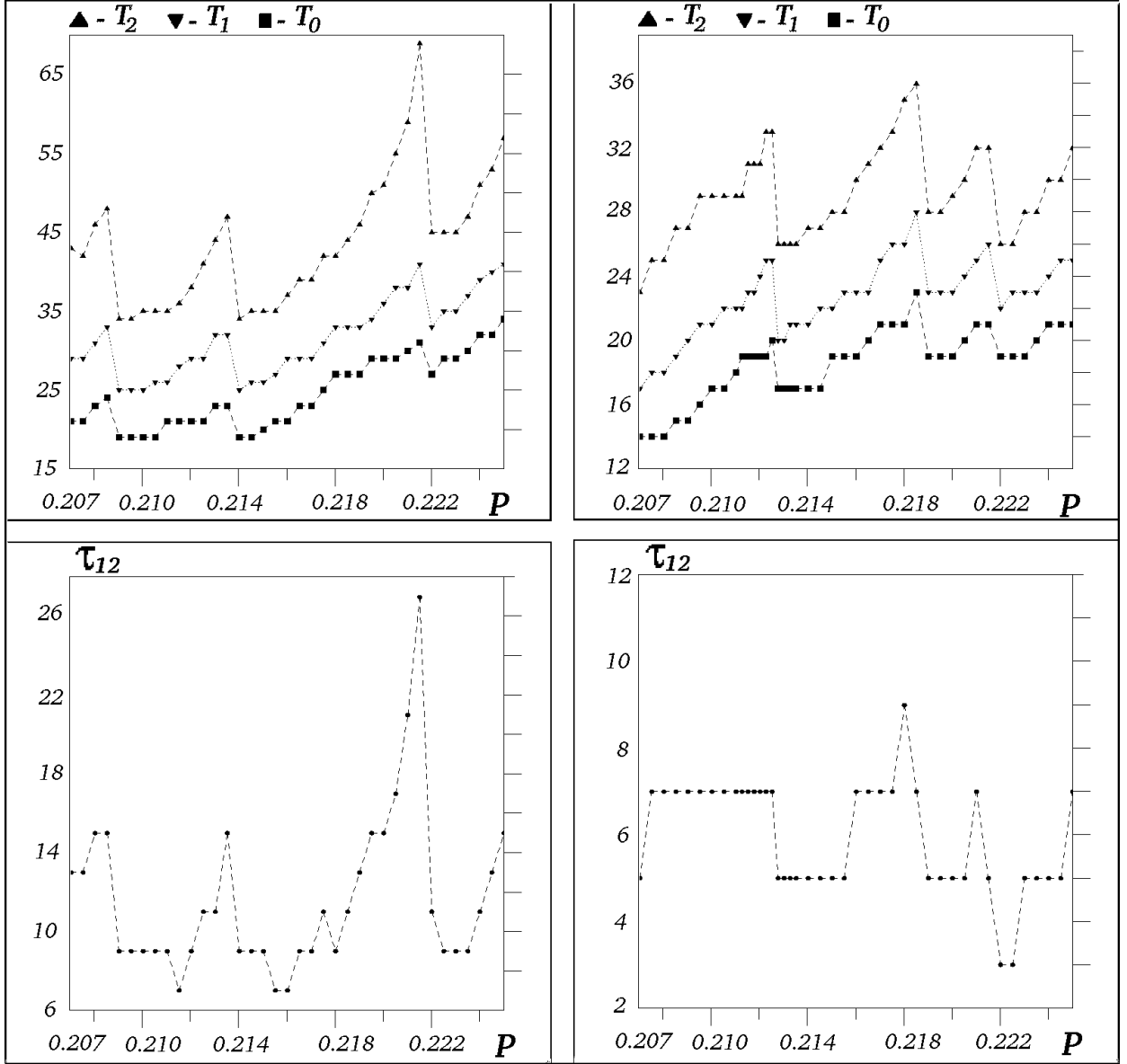


FIG. 9: Different degrees of harmony between distributions  $T_2(P)$  and  $T_1(P)$  which correspond to two ways of satisfying the condition of zero efficiency of the lattice order projecting onto REP (the example of the REP-ITP simulated with  $M = M_0$ ). Figures in the left column depict results obtained with this condition satisfied by random assigning all the possible arrangements of sites whose covering is allowed within vicinities  $V_x$  to all  $x \in \chi$ . The right column depicts the results obtained with  $\alpha = 0$  satisfied with preserving symmetry in arrangements of sites whose covering is allowed in  $V_x$  (this method is used here; see Section IV C and Ref. [17] for further explanations concerning the  $\alpha$ ).

tion transfer have reduced manifestations in the MMS patterns resulting from the REP simulations with the sufficiently large  $M$ . This reduction affects diversity of forms of increments in the MMS. The form of the  $\delta \int F_{T_j}$  is the one of manifestations of the F-SE which is relevant to opportunity for employing the REP simulations reported here to facilitate designing methods of regulating the collective effect accomplishment in corresponding real systems (see Section VI C). For this reason only, vanishing of this manifestation with growing  $M$  for the REP-ITP simulation series has been accepted here as cri-

terion being used to assess upper limit,  $M_1$  to the values  $M$  being moderate. Accordingly,  $260 < M_1 < 280$  has been identified by appearance of this qualitative change in the increments,  $\delta \int F_{T_1}$  and  $\delta \int F_{T_2}$ . The distributions  $T_j(M)$  detect here also certain value  $M^* \approx 220 > M_\tau$  such that with,  $M^* < M < M_1$ , the  $\delta \int F_{T_j}$  can be either scattered increments specific to the moderate  $M$  or may resemble the dispersed sedimentation-type increments.

Let us note, eventually, that results of REP-ITP simulations with  $M \approx M_1$  reveal manifestations attributed to the discreteness but they are remarkably weaker than

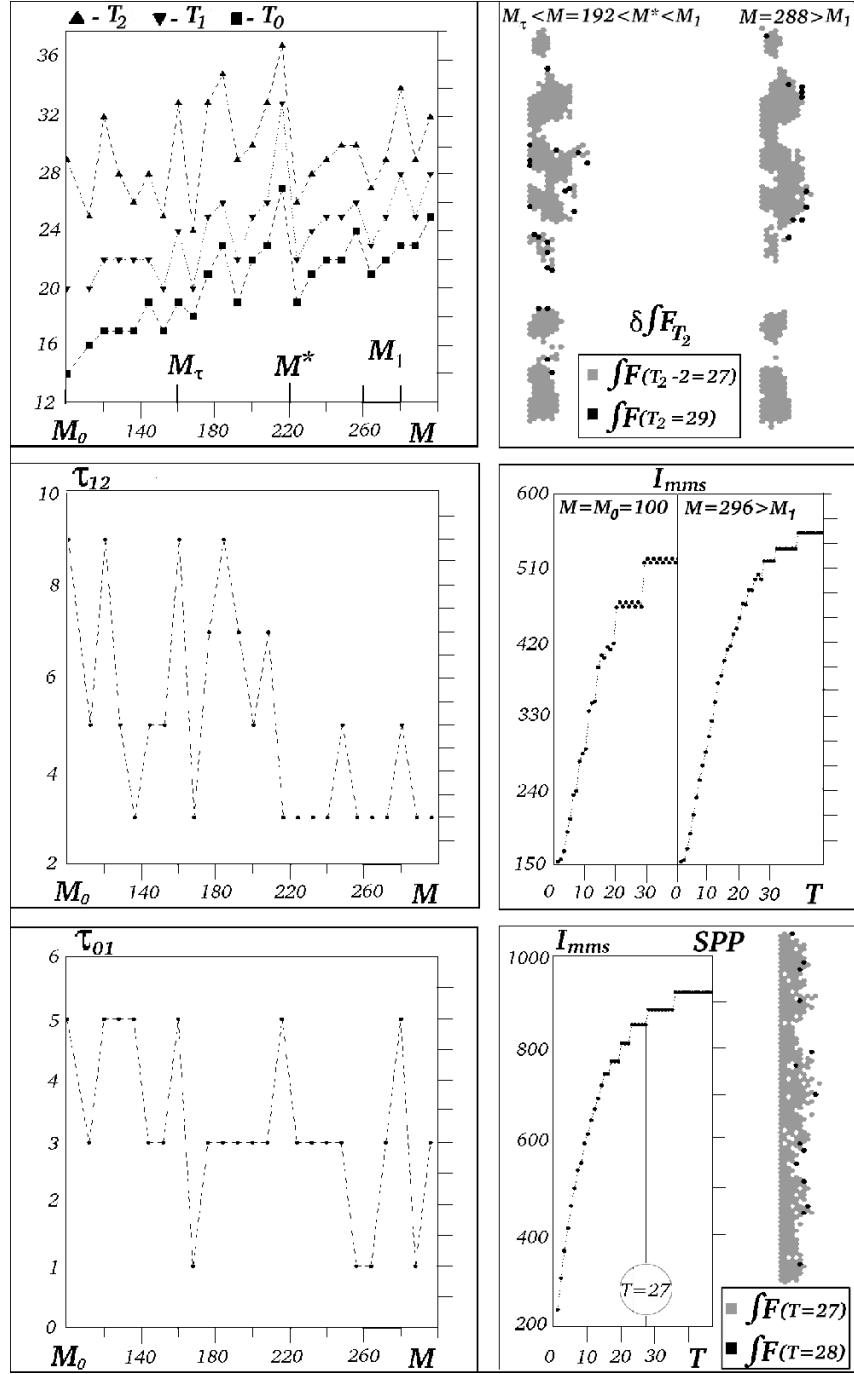


FIG. 10: Identifying the upper bound  $M_1$  of the  $M$  being moderate for example of the REP-ITP series with  $P=0.1311$ ,  $\alpha = \frac{1}{3}$ . For this example, a pair of distributions,  $I_{mms}(T)$  illustrates diminishing the effect of discreteness with growing  $M$ . Compare the increment  $\delta \int F_{T_2}(M > M_1)$  to the increment in MMS at jump in  $I_{mms}$  appearing in course of the SPP evolution (example of the SPP with  $P=0.475$ ,  $\alpha = \frac{1}{3}$ ,  $M = M_0 = 100$  is depicted by the indicated figure only). The figures depict bright pattern imposed on the black one.

those obtained with much lower moderate  $M \geq M_0$  (see Fig. 10). Although, the value of  $M_1$  depends on  $\alpha$  and  $P$ , the experience acquired shows that the  $M_1$  appears to be sufficiently high for performing reliable simulation series of the REP-ITP with varying  $P$ ,  $\alpha$  and  $M < M_1$ . Occur-

rence of the  $M_1$  has been detected for the REP-ITP and we have not observed the specific changes in  $\delta \int F_{T_j}$  for the REP-DTP simulated even with very high value  $M=600$ . Inspection of the REP-DTP and REP-ITP realizations in course of their evolutions explains this observation: Each

TABLE I: Dependence of increments in MMS on  $P$  and  $\alpha$  for REP-ITP. In the Tables,  $Si$  denotes sedimentation-type increment (see Fig. 6) which can be solid or dispersed; symbol  $\oslash$  identifies a null set or the increment being a single site covered whereas  $\sim\oslash$  shows that the increment is constituted by not more than  $2 \div 4$  not clustered covered sites (see Sections V, VIA, VIB for other denotations). The results presented have been obtained from simulations done with  $M = M_0$ .

scope of $P$	scope of P $P \rightarrow P^*$	for all $[P_a, P_b]$ within		
		$\frac{\delta f F_{01}}{(\delta f F_{10})} \mid \frac{\delta f F_{12}}{(\delta f F_{21})}$		
		$\alpha = 1$	$\alpha = \frac{1}{3}$	$\alpha = 0$
$P > P_T$	$P \rightarrow P_{b\ominus}$	$\frac{\sim\oslash}{(\oslash)} \mid \frac{\oslash}{(\oslash)}$	$\frac{\sim\oslash}{(\oslash)} \mid \frac{\oslash}{(\oslash)}$	$\frac{\sim\oslash}{(\oslash)} \mid \frac{\oslash}{(\oslash)}$
$P > P_T$	$P \rightarrow P_{a\oplus}$	$\frac{Si}{(Si)} \mid \frac{\oslash}{(\oslash)}$	$\frac{Si}{(\oslash)} \mid \frac{\oslash}{(\oslash)}$	$\frac{\sim\oslash}{(\oslash)} \mid \frac{\oslash}{(\oslash)}$
$P < P_T$	$P \rightarrow P_{b\ominus}$	$\frac{Si}{(Si)} \mid \frac{\oslash}{(\oslash)}$	$\frac{\sim\oslash}{(\oslash)} \mid \frac{\oslash}{(\oslash)}$	$\frac{\sim\oslash}{(\sim\oslash)} \mid \frac{\oslash}{(\oslash)}$
$P < P_T$	$P \rightarrow P_{a\oplus}$	$\frac{Si}{(Si)} \mid \frac{Si}{(Si)}$	$\frac{Si}{(\sim\oslash)} \mid \frac{\sim\oslash}{(\oslash)}$	$\frac{Si}{(\sim\oslash)} \mid \frac{\oslash}{(\oslash)}$

TABLE II: Dependence of increments in MMS on  $M$  for example of the REP-ITP with  $P = 0.1311$ ,  $\alpha = \frac{1}{3}$ , (then  $M_\tau = 160$ ) and REP-DTP with  $P = 0.104$ ,  $\alpha = 1$  (then  $M_\tau \approx 270$ ; see Table I for denotations).

$\frac{\delta f F_{01}}{(\delta f F_{10})} \mid \frac{\delta f F_{12}}{(\delta f F_{21})}$		
$M < M_\tau$	REP-ITP	$M > M_\tau$
$\frac{Si}{(\oslash)} \mid \frac{\oslash}{(\oslash)}$		$\frac{\oslash}{(\oslash)} \mid \frac{\oslash}{(\oslash)}$
$M < M_\tau$	REP-DTP	$M > M_\tau$
$\frac{Si}{(\oslash)} \mid \frac{Si}{(\oslash)}$		$\frac{Si}{(\oslash)} \mid \frac{\oslash}{(\oslash)}$

realization of the REP-ITP is constituted by chains of islands distributed rather uniformly in direction parallel to the initial structure (IS), however, some of realizations include narrow elongated tongues (see Fig. 3). For the very high  $M \approx M_1$ , this results in mean expected pattern revealing no changes within central part of the  $\int F$  at the jump. Then, only the frontal parts of the realizations are sufficiently diversified to contribute to the increment in the MMS. On the other hand, realizations of

the REP-DTP are split into two classes: Each realization in the class encompassing of about 70%  $\div$  80% of all the realizations forms only one or two big rugged clusters, situated against short subintervals of each IS chain, and few very small islands. Realizations constituting the remained part are represented by very small areas covered in their domains and resemble less developed realizations of the REP-ITP. Because of this diversification, reduction of the increment in the MMS at jumps to the form that would resemble this observed for the REP-ITP simulated with  $M \approx M_1$ , would require values of  $M$  much higher than the  $M_1$  detected for the REP-ITP.

### C. Discussion and conclusions

Series of the MMS patterns  $\int F(T)$  represents accomplishing the model collective effect in course of the REP. Discreteness of the REP results in a sequence of jumps in the MMS development during the process evolution. Modeling of the finite-size effects results in appearance of the structural bi-state. Using structural characteristics of the MMS pattern enables us to identify stabilization of the bi-state at the stage denoted as  $T_2$  which corresponds to certain jump (see Sections VB, VC). This  $T_2$  is the reference stage used in the search for specific changes in features of the MMS evolution pattern with varying the process parameters  $\{P, \alpha, M\}$ . The  $\tau_{01}$  and  $\tau_{12}$  separate the triplet of subsequent neighbor jumps in values of the MMS characteristics which occur in course

of the MMS development at stages  $T_j \in \{T_0, T_1, T_2\}$  (see Fig. 4). Occurrence of nonnull sedimentation-type increments and reductions in the MMS for the accumulation periods  $\tau_{01}$  and  $\tau_{12}$  is specific feature attributed to modeling the finite-size effects in the REP (see Fig. 6 and Tables I, II). Specific form of the scattered increments  $\delta \int F_{T_j}$  in the MMS development, which correspond to the jumps, is characteristic manifestation of the finite-size effects modeling in the REP. Reduction of this particular manifestation of the finite-size effects in a series of the REP-ITP simulations due to substantial reduction of the discreteness manifestations in the MMS patterns, which is observed with the sufficiently large  $M$ , corresponds to the upper bound  $M_1$  of the  $M$  being moderate. The lower bound  $M_0$  assures that all the REP realizations have no covered site in common and features of the corresponding MMS patterns are reliable.

Accordingly, the MMS evolution pattern  $\int F(T)$ , computed with the  $M$  being moderate  $M_0 \leq M < M_1$ , appears as sequence of bursts  $\delta \int F_{T_j}$  in series of patterns of the MMS increments. The patterns representing these bursts separated by the accumulation periods are constituted of sites scattered throughout whole the  $\int F(T_j)$ . This specific form of the increment  $\delta \int F_{T_j}$  enables us distinguishing the  $\delta \int F_{T_j}$  from neighbor increments for the accumulation periods by performing only observation of the MMS increment patterns (see Fig. 6).

In certain conditions parameterized by,  $\{P, \alpha, M\}$ , a burst  $\delta \int F_{T_j}$  separating an accumulation period with the sedimentation-type increment in the  $\int F$  from the following one with no or vanishing increment in the  $\int F$  can detect the  $T_1$ . Here, the examples of such conditions have been found by performing a number of series of the REP simulations (see Tables I, II). These results suggest that computing a number of series of the REP representing adequately a process underlying evolution of certain real system ensemble would enable us to predict parameters of real conditions corresponding to values of the relevant model parameters,  $\{P, \alpha, M\}$ . In those real conditions, stabilization of the structural bi-state of the  $\int F(T)$  recorded in course of the real process would be identified by observing the sequence of the bursts  $\delta \int F_{T_j}$  and increments in the MMS which may occur for periods between them. Note in this connection that identification of the increment in the MMS at a jump  $T_j$  or for the accumulation period refers to the same state of the bi-state that can be easily found in the simulation results. In a real system, performing this task may require more effort, particularly in situation when differences between states of the bi-state,  $\Delta \int F(T, T+1)$  are comparable to the increment in MMS at the jump,  $\delta \int F_{T_j}$ . However, for the jumps between the stabilized bi-states, the covered area representing the difference,  $\Delta \int F(T, T+1)$  is distanced from the front region of the expanding MMS whereas the increment,  $\delta \int F_{T_j}$  consists of elements occurring within whole the MMS (see Fig. 6 and Section V C 3). This difference between the sets noted is not observed for the pure ITP process, REP-ITP-P, in which stabilization of

the bi-state does not take place. Eventually, the feature just recalled would help detecting the  $T_2$  in real systems corresponding to the REP-ITP or REP-DTP. However, the distributions of the  $T_j(P)$  with other parameters fixed are much more regular for the REP-ITP than for the REP-DTP with lower  $M$  (see Fig. 8) and simpler with higher  $M$ . This makes real processes with scheme of information transfer corresponding to the REP-ITP the first candidates for the regulation. Thus results of the computations would enable us reducing a number of experiments required to realize the real process with regulating the collective effect accomplishment.

Let us emphasize that the opportunity just revealed appears for processes with accomplishing the bi-state enabling us detecting its stabilization events  $T_j$  whose role has been elucidated here previously. We have also shown that realization of transferring the information portions by the hopping finite-size elements is a prerequisite for appearance of the bi-state. Thus the opportunity aforementioned will not appear for processes without this kind of the information transfer.

Eventually, we *conclude*: Pattern of the MMS development, which represents accomplishing the model collective effect in course of the REP, experiences predictable changes with varying the parameters  $(P, \alpha, M)$  specifying the model ambient conditions.

This feature is attributed to modeling the finite-size effects in the REP simulation series.

For the REP-ITP, the effective prediction is possible with moderate number of realizations,  $M_0 \leq M < M_1$ .

#### D. Final remark

Let us recall that manifestations of the finite size effects (F-SE) appear to be a prerequisite for using changes in ambient conditions to regulate accomplishing the collective effect resulting from evolution of the ensemble of discrete systems. The F-SE result from fact that the local information transfer is realized with participation of elements represented by pairs of zero dimensional entities identified at the nearest sites of the array and experiencing conditional hopping to positions close by while transferring certain information portions and preserving their orientation in the space. Diversity of opportunities for realizing information transfers by the hopping pairs, which is much higher than for only distinct hopping zero dimensional particles, required effective modeling whose spatiotemporal aspect has been explained in Section II. This has enabled us to reveal the way of regulating the collective effect accomplishment.

On the other hand, it is known that certain evolutions of model discrete systems, whose all elements participating in the information transfer process allow considering them as zero dimensional particles only, may result in self-organizing structures composed of sites indicated in certain way in course of the process (see eg. Ref. [8]). However, the appearing structures do not start acting

as the hopping *functional* elements if no additional assumptions concerning that functioning in further course of the model process are made. This seems to suggest that the pairs representing the functional elements are required from the beginning of evolution of the ensemble systems to afford the opportunity for employing the ambient conditions to regulate the emerging collective effect in the way reported here. This particularly concerns the task of investigating the influence which changes in ambient determined factors can have on collective outcome of complex processes taking place in systems of the ensemble. The possible evolution of swarms of nanoelements mentioned here (see Sections I, II) as well as turbulent transport reported previously by us [9] may be considered as the examples of real processes for which this opportunity for investigating them appears to be useful.

### APPENDIX: MEAN MEASURE SET REPRESENTATION

Below, we present only brief technical way, in which the mean measure set representation, MMS is computed; the relevant theory is given in [11].

The MMS, denoted here also as  $\int F$  has been proposed [11] for characterizing mean expected form of a finite random set  $F = \{A_i, i = 1, 2, \dots, M\}$  constituted by finite number  $M$  of its realizations  $A_i$ ,

$$\int F = \{\Phi_M > h\}^1 \cap \{\Phi_M < h\}^0, \quad (\text{A.1})$$

with the value  $h \in [0, 1]$  given by the inequalities,

$$\mu\{\Phi_M > h\} \leq \frac{1}{M} \sum_{i=1}^M \mu\{A_i\} \leq \mu\{\Phi_M \geq h\}, \quad (\text{A.2})$$

where  $\in$  is read "is an element of",  $\mu\{\cdot\}$  denotes the

number of elements of the set  $\{\cdot\}$ ,  $\{\Phi_M > h\}$  is a set of such elements  $x \in \chi$  that  $\Phi_M(x) > h$  and symbols  $\{\cdot\}^0$ ,  $\{\cdot\}^1$  denote set-theoretical cells determined in respect to a set  $\{\cdot\}$ . A cell of empty conjunction,  $D^0 = \{\mathcal{A} \subset \mathcal{M} : \mathcal{A} \cap D = \emptyset\}$  and the cell of inclusion,  $D^1 = \{\mathcal{A} \subset \mathcal{M} : \mathcal{A}^c \cap D = \emptyset\}$  are defined as classes of finite sets  $\mathcal{A}$  in the space  $\mathcal{M} = 2^\chi$  of all subsets of the space  $\chi$ , in respect to elements  $D$  of the set  $\mathcal{D}$  covering the space  $\chi$  where,  $\mathcal{D} = \{D_j \subset \chi, j = 1, 2, \dots, N_{\mathcal{D}}\}$  and  $D_k \cap D_j = \emptyset \forall j \neq k$ . Here,  $\mathcal{A}^c$  denotes complement of the  $\mathcal{A}$  to  $\mathcal{M}$ , symbol  $\emptyset$  denotes a null set,  $\forall$  is read "for all",  $\cap$  and  $\subset$  denote common part and inclusion of sets, respectively. The  $\Phi_M = \Phi_M(x)$  is the mathematical expectation,

$$\Phi_M(x) = \frac{1}{M} \sum_{i=1}^M \Phi(x, A_i), \quad (\text{A.3})$$

with  $\Phi(x, A_i) = 0$  if  $A_i \in \{x\}^0$  and  $\Phi(x, A_i) = 1$  if  $A_i \in \{x\}^1$ , where  $\{x\}$  is the single element set. Uniqueness of the canonical cell representation Eqs. (A.1) has been proved [11]. The multitude of sets  $\int F$  is represented unambiguously by its single component: if  $h \geq 0.5$  one takes the one whose measure is largest; if  $h < 0.5$  one takes the one whose measure is smallest [11]. In this work, only such single set representation is used so it is denoted in the text by  $\int F$  or MMS.

### ACKNOWLEDGMENTS

The parallel computations have been performed by using computer Cray-T3E with computational grant at The Interdisciplinary Centre for Mathematical and Computational Modelling at The Warsaw University; Partial support from Polish-British Research Partnership Programme WAR/341/202 and NATO Collaborative Linkage Grant PST.CLG.976545 is acknowledged.

- 
- [1] R. E. Smalley, *Angew. Chem.* **36**, 5000 (1997).
  - [2] J. Liu et al., *Science* **280**, 1253 (1998).
  - [3] Z. Liu et al., *Langmuir* **16**, 3569 (2000).
  - [4] A. K. Boal and V. M. Rotello, *J. Am. Chem. Soc.* **122**, 734 (2000).
  - [5] C. J. Kiely et al., *Nature* **396**, 444 (1998).
  - [6] M. Brust, C. J. Kiely, D. Bethell, and D. J. Schiffrin, *J. Am. Chem. Soc.* **120**, 12367 (1998).
  - [7] P. W. Anderson, *Phys. Rev.* **109**, 1492 (1958).
  - [8] S. Wolfram, *Rev. Mod. Phys.* **55**, 601 (1983).
  - [9] W. Kozłowski, *Int. J. Num. Meths. Fluids* **23**, 105 (1996).
  - [10] B. Mayer and S. Rasmussen, in *Proceedings of Sixth International Conference on Artificial Life, Los Angeles UCLA, USA, June 1998*, edited by K. Adami, Belew and Taylor (MIT Press, Cambridge, 1998).
  - [11] O. Y. Vorobev, *Mean-Measure Modeling* (Nauka, Moscow, 1984).
  - [12] D. Hilbert and S. Cohn-Vossen, *Anschauliche Geometrie* (Springer-Verlag, Berlin, 1999).
  - [13] F. James, *Comput. Phys. Commun.* **60**, 329 (1990).
  - [14] M. Luscher, *Comput. Phys. Commun.* **79**, 100 (1994).
  - [15] F. James, *Comput. Phys. Commun.* **79**, 111 (1994).
  - [16] K. Janich, *Topology* (Springer-Verlag, New York, 1984).
  - [17] W. Kozłowski, *Comput. Phys. Commun.* **143**, 155 (2002).
  - [18] H. F. Harmuth, *Information Theory Applied to Space-Time Physics* (World Scientific, Singapore, 1993).